

# ***Ionization-based detectors and low-noise techniques: six decades of contribution to the advancement of physics***

**Pier Francesco Manfredi**

**Lawrence Berkeley National Laboratory - Berkeley, California (USA)**

**[pfmanfredi@lbl.gov](mailto:pfmanfredi@lbl.gov)**

## OUTLINE

- ❖ The ionization-based detectors
- ❖ Ionization chambers
- ❖ The advent of solid state detectors
- ❖ Stochastic noise and its effects
- ❖ Segmented detectors for position sensing
- ❖ Back to the origin
- ❖ Conclusions
- ❖ Appendix

# ***The ionization-based detectors***

Throughout this talk the discussion is restricted to detectors that have two salient features:

- ❖ Ionization is their basic sensing mechanism
- ❖ No built-in charge multiplication process is present

This is quite a broad category of detectors, as it includes:

**Ionization chambers using gaseous, liquid and solid sensitive regions.** Gas-filled ionization chambers, calorimeters employing cryogenic liquids and solid-state detectors employing insulators, for instance diamond, belong to this group.

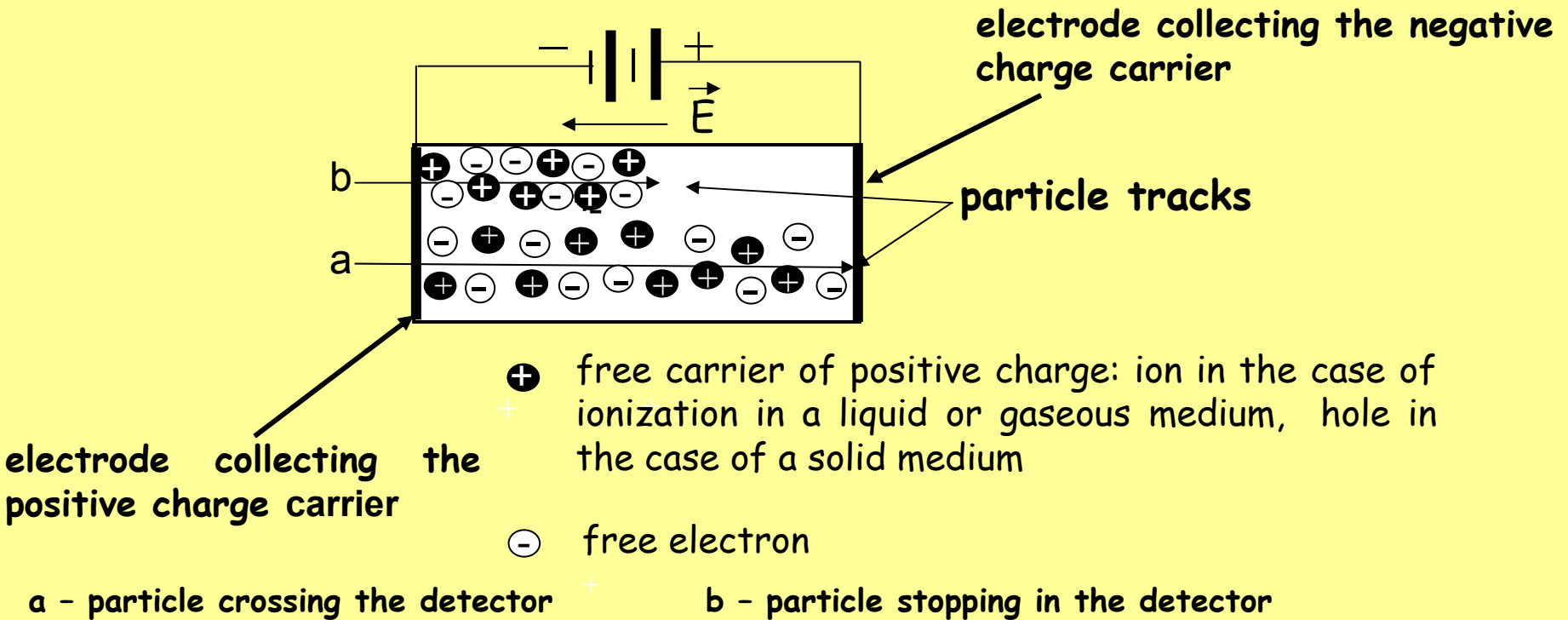
**Semiconductor detectors** based on different materials and of different geometric structures, including highly segmented units also fall into this group.

**For all these detectors, the absence of a built-in charge multiplication has the consequence that the contribution to the useful signal is due solely to the primary ionization charge,** which can be small, down to some hundreds of femtocoulomb in the least favorable cases.

Two aspects will be addressed:

- the intervention of these detectors in physics research
- the expertise their development and their use conveyed to the instrumentation techniques

The basic structure of an ionization-based detector is shown in the figure below. Two electrodes are inserted in the sensitive medium and a bias voltage source is applied between them. The figure shows the ionization tracks determined by the incoming radiation



The electric field created by the bias voltage supply inside the sensitive region has a twofold purpose. **It avoids the recombination of the free carriers and makes them drift** toward the relevant collecting electrodes

A fundamental parameter of the material employed in the sensitive region of an ionization detector is the energy  $\varepsilon$  (eV) required to create a pair of carriers. ***The smaller is  $\varepsilon$  the larger is the number  $N$  of pairs, the larger and therefore less likely to be deteriorated by external unwanted effects is the useful signal provided by the detector.*** For the sake of comparison, Germanium features a value of  $\varepsilon$  smaller by about a factor 10 than the value in Argon, the gas more frequently used in ionization chambers.

***The detector information is contained in the currents induced by the carriers*** in their drift motion towards the collecting electrodes. For instance, the energy released by the incoming radiation in the sensitive volume is proportional to the charge associated with the induced currents. Therefore, an energy measurement implies a charge evaluation, that is, ***the integration of the induced current signal.***

The shapes of the currents depend on the nature of the detector and on the material employed in their sensitive region. However, the following two considerations are of general validity.

- ***Both types of carrier induce current on both electrodes***
- ***The induction process ends only when all carriers are collected***

Consequence of the last statement is that in accurate charge measurements, like energy spectrometry, that require the total charge collection to have an information strictly dependent only on the energy deposited, the ***operational time of the detector is determined by the collection time of the carriers of lower mobility.***

Suppose now that a strictly monochromatic radiation falls on the detector and that the amplitude spectrum of the signals appearing at the output of the conditioning system is accumulated. A delta-impulse-like spectral line would be expected. Instead, a gaussian distribution of finite width would appear. Several physical processes contribute to the width of the observed line. Let  $\sigma$  be the standard deviation of the gaussian distribution and FWHM its full width at half maximum. The following relationship holds:

$$\text{FWHM} = 2.355 \sigma$$

Calling  $\sigma_1, \sigma_2, \dots, \sigma_n$  the standard deviations due to the single processes, that are generally statistically independent from each other:

$$\sigma^2 = \sigma_1^2 + \sigma_2^2 + \dots + \sigma_n^2$$

Some contributions to  $\sigma^2$  have their origin in the detector and are related to the nature of the interaction of the radiation with the detector, Some other ones are due to defects in the detector. The signal processing electronics is responsible for additional line broadening, a very important contribution of which is due to noise in the front-end.

## FUNDAMENTAL SOURCES OF SPECTRAL LINE BROADENING IN ENERGY MEASUREMENTS

- Consider the case of an ionization detector made of an extremely pure material and manufactured in an ideal way, so to have an extremely thin entrance window.
- Suppose also the radiation source to be extremely well collimated, so that the radiation enters the detector at a fixed angle.
- Suppose finally that the intensity of the source is so low that the effects of high counting rate on the width of the spectral line are totally negligible.

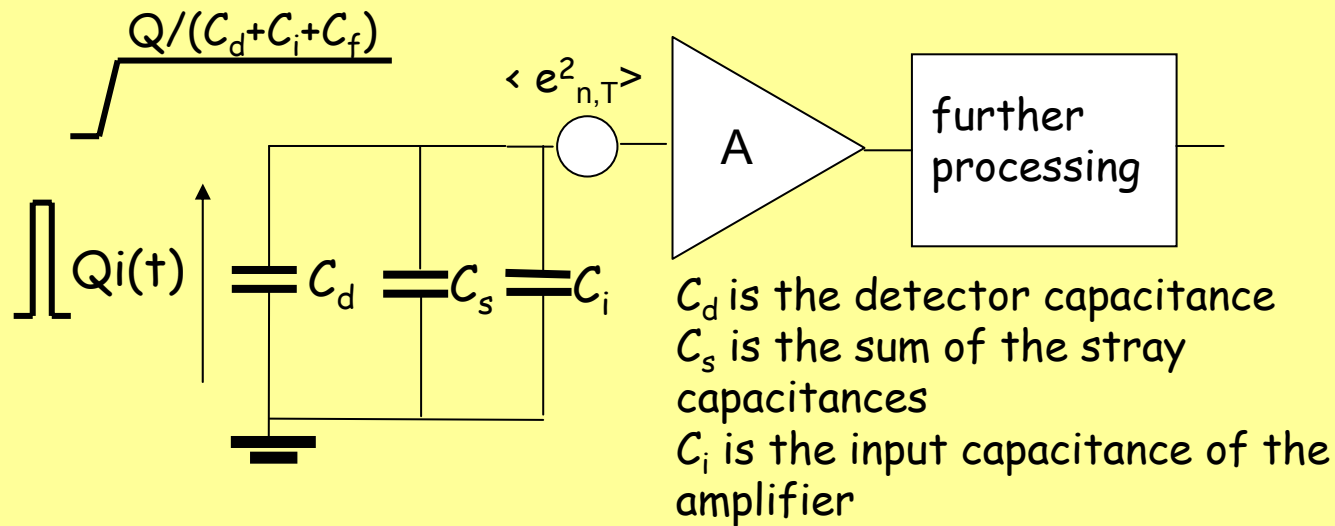
**These are the ideal conditions for a high resolution spectrometry.**

Still, sources of line broadening exist and they set the fundamental limit to the resolution.

**One is the fluctuation in the number of pairs created by the radiation.**

The statistics of pair creation in the ionization process features a standard deviation lower than the one relevant to a Poisson distribution. If the statistics were poissonian, the variance  $\sigma^2$  on the number of carriers created when the energy  $\mathcal{E}$  is deposited,  $N = \mathcal{E} / \varepsilon$  would be equal to  $N$ . Instead, the process of pair creation by ionization exhibits a variance reduced by the factor  $F$ , the Fano factor:  $\sigma_1^2 = FN$  with  $F < 1$ , that is,  $\sigma_1^2 = F\mathcal{E}/\varepsilon$  or, referred to the energy,  $\sigma_1^2 = \varepsilon F\mathcal{E}$

The **second one** is related to the need of converting the charge delivered by the detector into an electrical variable of sufficient amplitude to enable the final processing steps, like, for instance, the analog-to-digital conversion. To grasp the nature of the problem in a nutshell, refer to the oversimplified situation of the figure. **The schematics describes how the detector charge can be converted into a voltage by integration on the sum of detector capacitance and the other capacitances shunting it, a solution which is feasible as long as  $C_d$  is reliable in value.** The resulting voltage  $Q/(C_d+C_s+C_i)$  is presented to the front-end amplifier. The root-mean square voltage  $\langle e^2_{n,T} \rangle$  represents the total input-referred noise of the amplifier. **The noise considered in what follows is intimately related to the devices that constitute the amplifier system. It is due to spontaneous fluctuations of matter and electricity and cannot be eliminated even by the most advanced engineering skill.**



This figure shows the principle of charge measurement with any ionization-based detector.

The charge variance due to the front-end noise is:

$$\sigma^2_2 = (C_d + C_s + C_i)^2 \langle e^2_{n,T} \rangle \text{ and in terms of energy } \sigma^2_2 = \varepsilon^2(C_d + C_s + C_i)^2 \langle e^2_{n,T} \rangle .$$

**Therefore, the lowest limit achievable** in the spectral linewidth is expressed by:

$$\text{FWHM}_{\min} = 2.355 [ \varepsilon F \mathcal{E} + \varepsilon^2(C_d + C_s + C_i)^2 \langle e^2_{n,T} \rangle ]^{1/2}$$

The previous equation shows that with the same noise contribution from the front-end amplifier, **at a higher energy deposited in the detector, the minimum achievable FWHM is governed by the statistics in the pair creation, while at a lower energy deposited the front-end noise would take over.**

For instance, in the energy measurements of the highest resolution, the spectral analysis of X and gamma rays with semiconductor detectors, **with X rays** of a few keV, **the front-end noise is an issue of the highest importance.** Instead, with **gamma-rays** in the 1 MeV energy region, the larger contribution to the spectral linewidth comes from the **statistics in the pair creation.**

The analysis done so far is oversimplified as only the noise in the front-end device is considered . More insight into the subject will be given later on.

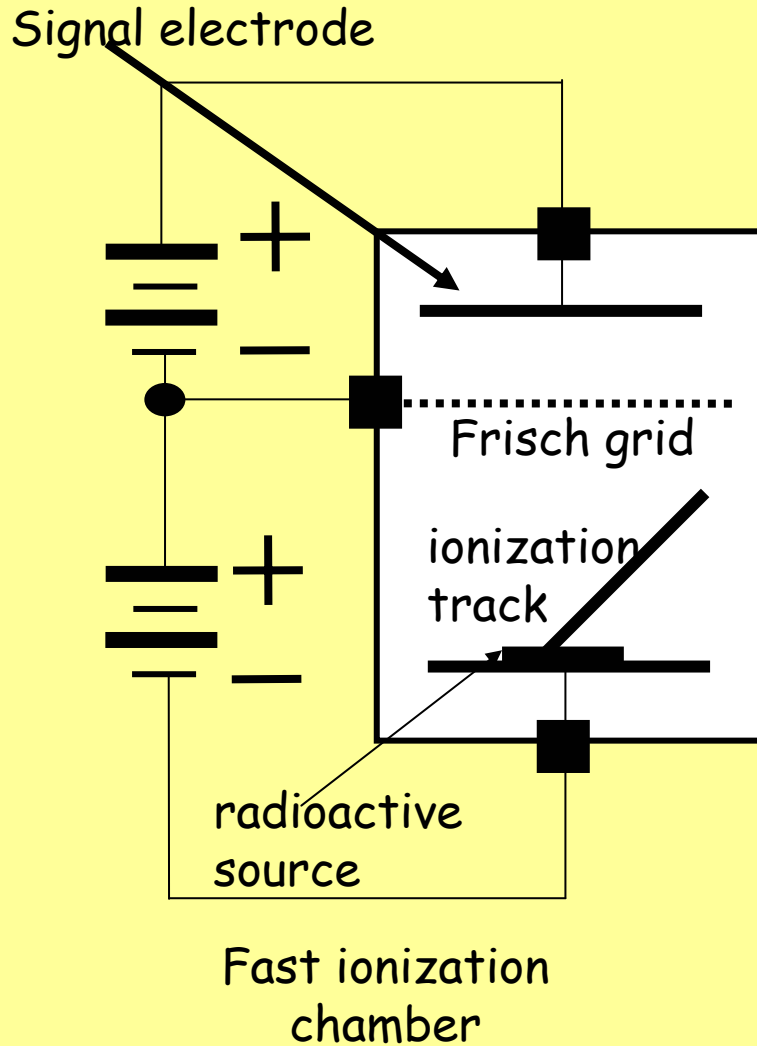
# ***Ionization chambers***

The term ionization chambers should be restricted to those ionization-based detectors whose sensitive region between the electrodes is made of a **structurally homogeneous** material. Examples of detector of this nature are:

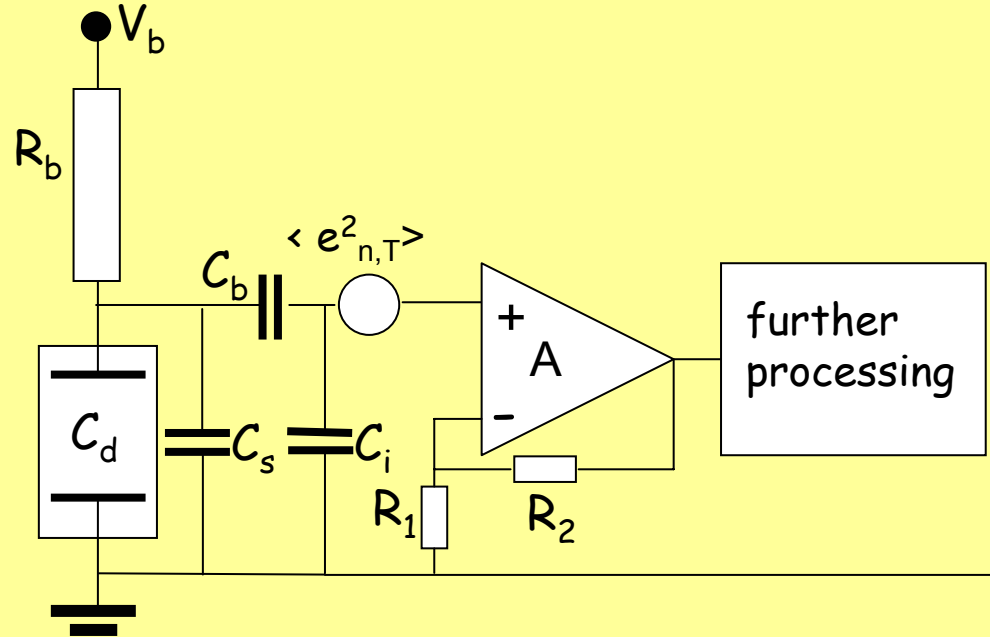
- the gas-filled ionization chamber
- the ionization chambers based on a liquid, among them the gaps of liquid calorimeters
- the ionization chambers based on a solid insulator, for instance the diamond detector

Semiconductor-based detectors, that are realized as P-N junctions or Schottky-barrier junctions, are ionization-based, but do not consist of a **structurally homogeneous** region.

The gas-filled ionization chamber.



The chamber drawn in the figure was an advanced version employing a grid to prevent the induction on the signal electrode by the low mobility carriers (positive ions).



Before the advent of the charge-sensitive loops the induced current was integrated on the total capacitance  $C_d + C_s + C_i$  and the resulting voltage amplified by a voltage-sensitive amplifier

The gas-filled ionization chambers still have several applications. One, which is very important and related to an extremely recent achievement of physics will be shortly described toward the end of this talk.

In the history of modern physics, **they provided a noticeable contribution to the knowledge of the energy spectra of  $\alpha$  particles emitted by natural radioactive substances.** Besides pure science and applications, the gas-filled ionization chambers had a remarkable importance also in the advancement of instrumentation as underscored by the following considerations:

- They raised the issue of the noise limitations in detector measurements
- Related to them was the discovery of the sub-poissonian nature of the statistics of pair creation in the sensitive medium (Fano, 1947).
- The Frisch-grid principle of getting rid of the charge induction due to slowly drifting carriers is likely to have suggested to Paul Luke a method of avoiding the contribution to the induced signal by the low-mobility holes in CdTe detectors (principle of Coplanar Grids).

## IONIZATION CHAMBERS BASED UPON SOLID MEDIA

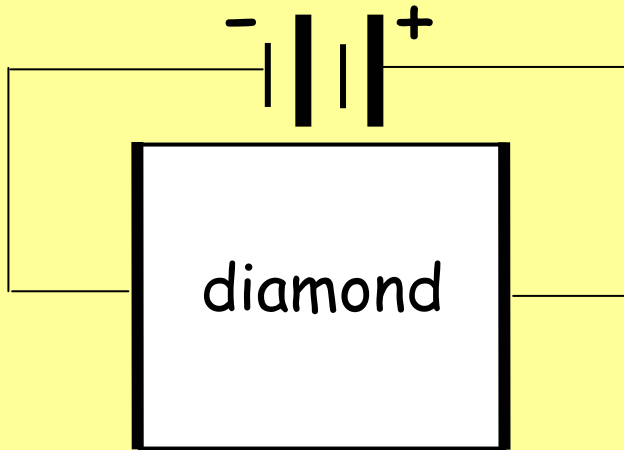
The attempt to use a solid material in the sensitive region of an ionization chamber responds to the obvious need of increasing the density in that region beyond the values that can be achieved by filling the chamber with a pressurized gas.

A detector which, strictly speaking, reproduces the structure of the ionization chamber discussed so far, would work as long as the material employed in the sensitive region is an insulator or a semiconductor featuring a large energy gap in its band model. For instance, *diamond detectors are classical ionization chambers.*

*The idea would fail if the material were a semiconductor like germanium or silicon or any other semiconductor with an energy gap of 1 or 2 eV.* The reason is that under applied voltage the current flowing across the sensitive region and the statistical fluctuations associated with it **would mask** the small currents induced on the electrodes by the carriers created by the radiation to be detected.

The solution to the problem was found by realizing the detector as a P-N, diode-like junction, and operating it in the reverse-biased mode, as will become clear in the section on semiconductor detectors.

The figure below shows a diamond detector as an example of an ionization chamber employing a solid medium. It is realized by evaporating the electrodes on the opposite faces of a slab of diamond. Diamond ionization chambers were proven to be very good detectors in energy spectrometry of  $\alpha$  particles, of  $\beta$  rays in the 100 keV energy region, in  $dE/dx$  measurements on Minimum Ionizing Particles (MIPs). The value of  $\varepsilon$ , the energy required to create an electron-hole pair in diamond is 13.2 eV, nearly four times larger than in silicon (3.6 eV). However, the dielectric time constant of diamond is nearly half that of



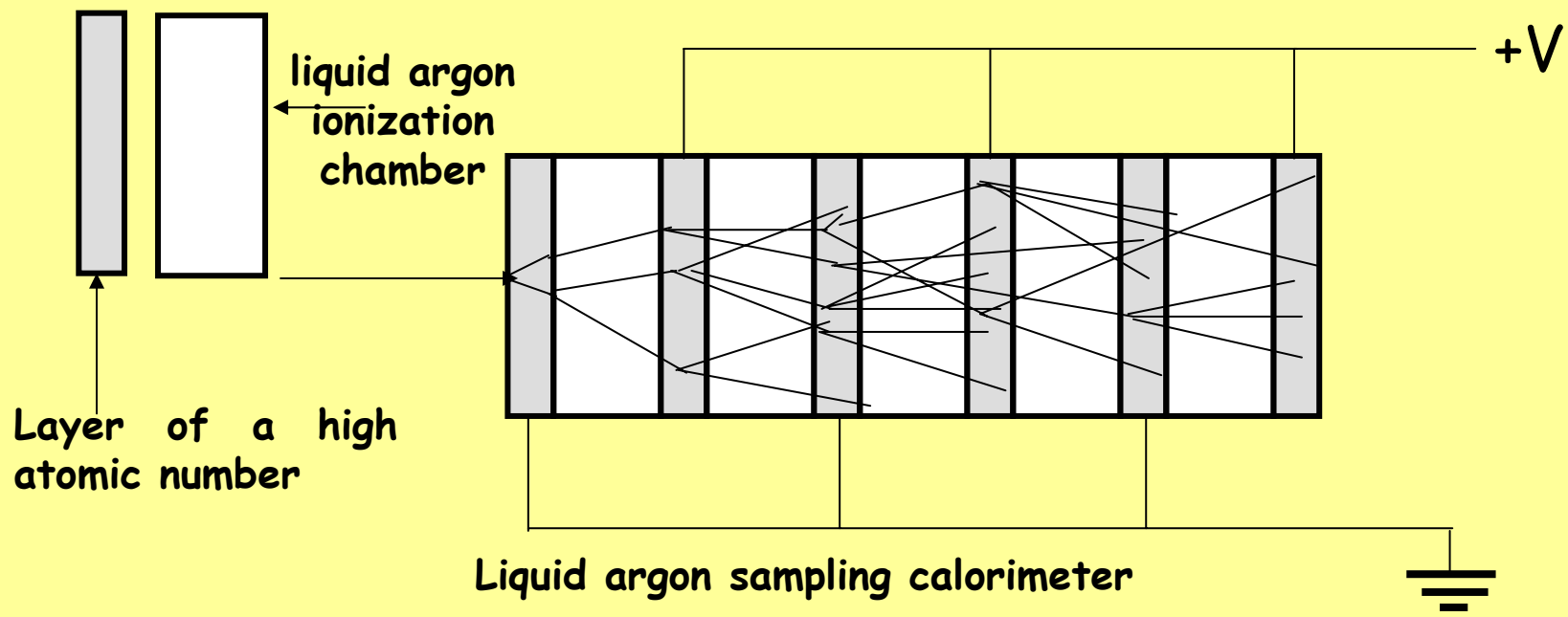
silicon, so the ratio which matters,  $\mathcal{E}/\varepsilon C_d$  for a

silicon and a diamond detector of equal geometry at the same energy released  $\mathcal{E}$  is only a factor 2 in favor of silicon.

***Diamond is more radiation tolerant than silicon, and easier to be configured in segmented structures.*** By virtue of this, it is being looked at with a great interest as a suitable material for detector applications at high luminosity colliders. In the framework of the ***LHC R&D activities, the RD 42 collaboration*** was established with the aim of investigating the possibility of using diamond in microstrip and pixel implementation for vertex detectors and trackers.

## IONIZATION CHAMBERS BASED UPON LIQUID MEDIA

Ionization chambers filled with cryogenic liquids, like liquid Ar, Liquid Kr, liquid Xe are of great importance. As compared to the gas filled ionization chambers, the positive ions in a liquid can be considered virtually immobile, so that the induced current is evaluate taking into account only the contribution of the electrons. Each gap in the calorimeter shown below behaves as an ionization chamber



The importance of calorimeters based on cryogenic liquids in elementary particle physics is very well known and it wouldn't make sense to discuss it here. It is more useful, instead, to discuss their fallout on low-noise front-end techniques.

One of the issues the advent of liquid argon calorimeters brought up was related to the **large capacitance, thousands of picofarads, presented by the gaps to the front-end electronics**. It must be remembered that all active elements are charge-controlled devices and a high resolution charge measurement in the presence of noise **requires an optimization in the charge transfer from the detector to the active device in the front-end**. This condition is met by the so called **capacitive matching**, which has become a basic point in low-noise techniques.

When the liquid argon calorimeters made their appearance on the scene of elementary particle physics in the early seventies, the available low-noise field-effect transistors were rather small devices, featuring comparatively low values of input capacitance and transconductance. The optimization in the charge transfer was based upon matching transformers. Only years later, when the collaboration between experimenters and microelectronics foundries became feasible, the development of special junction field-effect transistors tailored to applications with detectors of very large capacitance, like *Interfet NJ 3600*, became possible.

One more interesting contribution brought about to low-noise techniques by cryogenic-liquid calorimeters was in the area of front-end circuits able to operate at the temperature of the cryogenic liquids, basically LAr and LKr. Valuable studies about front-end solutions for cryogenic operation were done at Brookhaven lab in the framework of ATLAS LAr calorimeter as a collaboration between Brookhaven and the INFN extensions of Milan and Pavia.

# ***The advent of solid state detectors***

A historical document, 1960

Semiconductor  
Nuclear Particle Detectors

Proceedings of an Informal Conference  
Asheville, N. C., September 28-30, 1960

J. W. T. Dabbs and F. J. Walter, Editors

Publication 871  
National Academy of Sciences—National Research Council  
Washington, D. C.  
1961

SESSION I

C. J. Borkowski, Chairman

BASIC MECHANISMS OF OPERATION

1. Pulse Formation In Semiconductor Detectors

J. W. Mayer

I would like to discuss in a very general way the operation of semiconductor junction detectors primarily to illustrate the salient features that will affect the performance of these units.

The present work is an outgrowth of work done by Van Heerden, Chynoweth and others on crystal counters<sup>(1)</sup>. Consider a high resistivity material across which an electric field has been applied. Electron-hole pairs created by the incident charged particles will separate and drift under the action of the field (Fig. 1). The motion of the carriers induces a charge on the electrodes proportional to the fraction of the voltage drop the carriers traverse<sup>(2)</sup>.

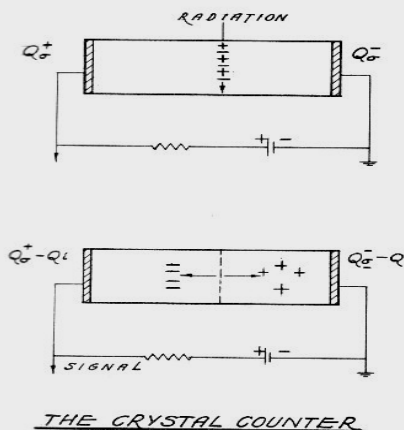


Fig. 1. (a) Crystal counter with voltage applied. An incident charged particle creates electron-hole pairs. (b) Motion of the charge carriers induces charge on the end plates, producing an external signal.

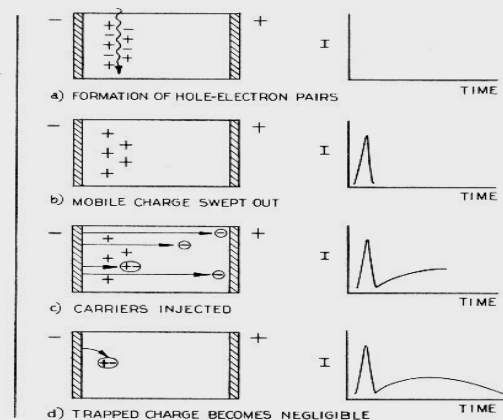


Fig. 2. Crystal counter in which only the electrons are mobile. The presence of positive immobile charge causes electron injection.

Semiconductor detectors in their basic structures were **P-N junctions made of a thin, highly doped (P+) region diffused or implanted into a lightly doped (N-) region**. Upon application of a reverse bias voltage to this junction the region of light doping becomes depleted by removal of mobile carriers. The N- region acts as the sensitive region of the detector and if the reverse voltage reaches a sufficient magnitude, **the N- region becomes totally depleted**.

Operation in total depletion is **an almost ideal condition**, for the sensitive region spans the entire longitudinal dimension of the detector while the detector capacitance becomes independent of any further increase in the bias voltage. This, for instance, leaves more freedom in the choice of the front-end preamplifier (see **Voltage-Sensitive or Charge-Sensitive Preamplifier?** in the appendix).

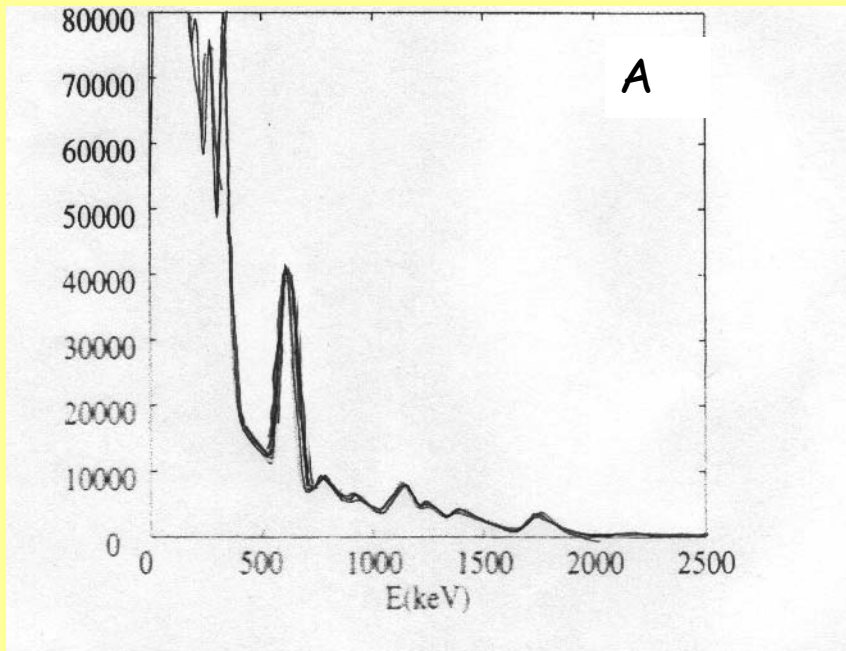
Alternatively, junction-based semiconductor detectors were realized as Schottky-barrier devices and for some materials this technology is still employed.

Already in the early days of semiconductor detectors it became clear that the described technologies couldn't allow the realization of depletion layers of sufficient depth to detect, for instance, gamma-rays in the 1 MeV energy region. **The technology of Lithium drift was introduced**. It consists in initially diffusing Lithium, which behaves as a pentavalent impurity, into a slab of P-type material (Ge or Si). Under application of an electric field, Li, which drifts through the P region, makes it almost intrinsic by compensating the original P-type impurity. The Lithium-drift approach was employed with Germanium and Silicon. In Germanium it was superseded by the appearance of High Purity material (HPGe), while for silicon it is still in use.

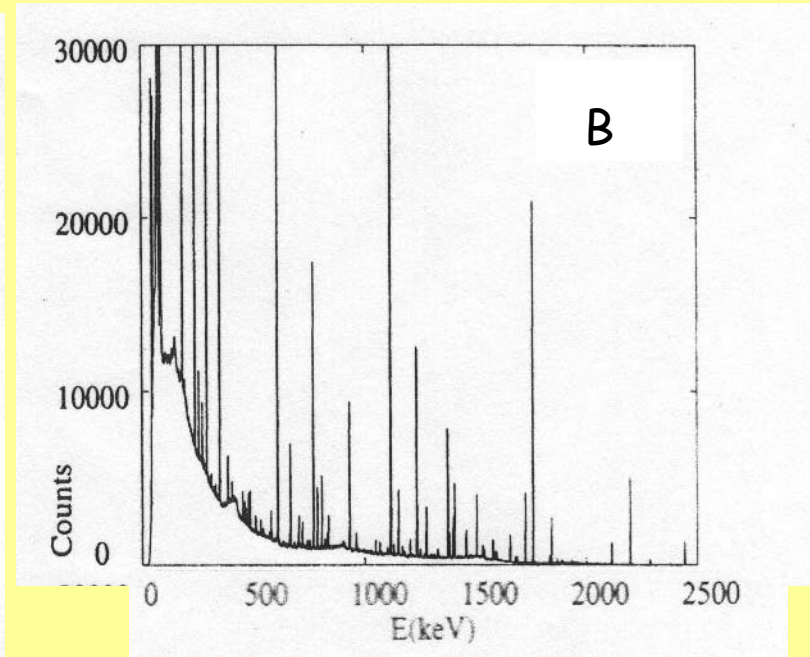
## DOMAINS OF APPLICATION OF SOLID STATE DETECTORS MADE OF DIFFERENT MATERIALS

**GERMANIUM** - *By virtue of its high  $Z$  (32) it is employed in high resolution gamma-ray spectrometry. It also features a high mobility of both carriers, enhanced by the operation in cryogenic condition, which is necessary to reduce the detector leakage current. Nowadays Ge detectors are realized as junction structures on High Purity material (HPGe). (For best resolution they are ordinarily operated at liquid Nitrogen temperature,  $T=77$  K)*

Prior to the advent of semiconductor detectors, gamma-ray spectrometry relied on NaI and CsI scintillation detectors. The energy resolution was poor, being limited by the statistics in the scintillation and charge multiplication processes.



$^{226}\text{Ra}$  gamma-ray spectrum from a  $309\text{ cm}^3$  NaI detector



$^{226}\text{Ra}$  gamma-ray spectrum from a  $240\text{ cm}^3$  coaxial germanium detector

The germanium detectors, initially  $\text{Ge}(\text{Li})$ , later  $\text{HPGe}$ , brought about a dramatic improvement in the resolution of  $\gamma$ -ray spectrometry, as it can be inferred by comparing figures A and B.

***SILICON*** - Besides being the best detector material for X-rays up to energies of about 10 KeV, silicon covers a broad variety of other applications, among them:

- spectrometry of charged particles ( $\alpha$  and  $\beta$ ), of fission fragments
- dE/dx measurements on minimum ionizing particles in particle physics

The structure obtained by ion-implanting P impurities on a high resistivity N-type material has undergone a remarkable technological improvement in the early eighties when ***the planar process currently employed in microelectronics was introduced in the detector fabrication.***

Detectors obtained in this way have thicknesses ranging from tens of microns to a few millimeters

***LITHIUM DRIFT on SILICON*** is the process employed to obtain detectors with a thick (up to 1 cm) nearly intrinsic region. These detectors are the choice solution for the spectrometry of X-photons at energies up to 100KeV. They require cryogenic operation for best performances.

***The silicon drift detectors***, that will be discussed later, have opened up the possibility of a high resolution X-ray analysis at room temperature, which is made possible by their particular structure associated with a front-end device realized directly on the high resistivity detector chip.

## ***CADMIUM TELLURIDE CdTe and CADMIUM-ZINC-TELLURIDE CdZnTe***

Are materials of a high atomic number and as such can be utilized for gamma-ray detection. Besides, their comparatively large  $E_G$  allows the operation at room temperature or at a moderate cooling. Its limitations are:

- Low mobility of both carriers, in particular of the holes.
- Limited purity level of the material, therefore presence of traps
- Non negligible leakage current, particularly in CdTe.

A remarkable improvement in their spectroscopic behavior has been brought about by the introduction of the Coplanar Grids (P.N. Luke, 1994)

P.N. Luke, **Single-polarity charge sensing in ionization detectors using coplanar electrodes.** *App. Phys. Lett.* 65, pp2884-2886, 1994

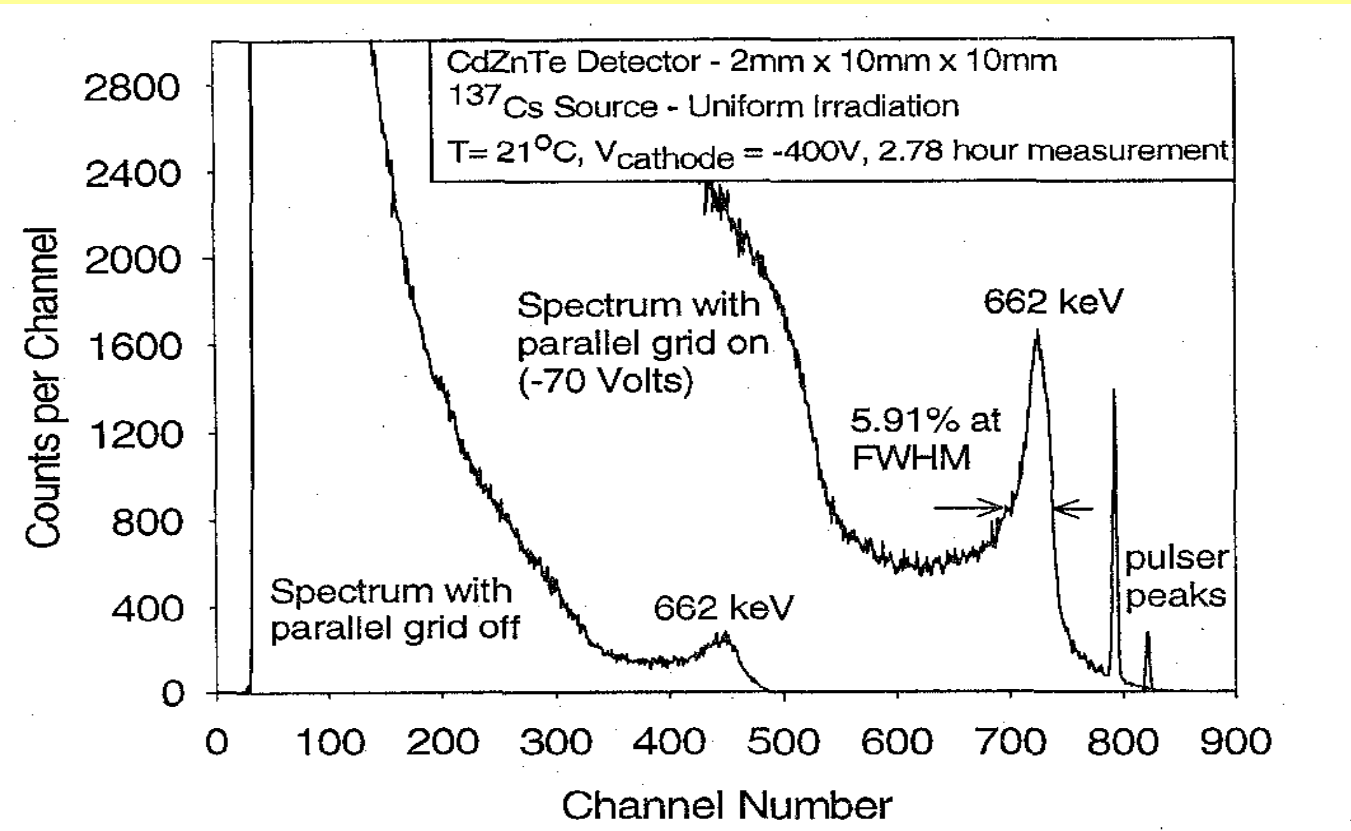


Figure 12. Room temperature spectra of 662 keV gamma rays from the 10mm x 2mm x 10mm CdZnTe semiconductor parallel strip Frisch grid detector with the grid off (floating) and on (-70 volts).

D.S.Mc Gregor et al - CdZnTe Semiconductor Parallel Strip Frisch Grid Radiation Detectors - IEEE Trans.,Nucl.Sci, 45,3, June 1998

# ***Stochastic noise and its effects on measurements with ionization-based detectors***

## Noise in passive components:

### Thermal noise in resistors

First observed by J.B. Johnson in metal resistors. Original paper:  
J.B. Johnson: Thermal agitation of electricity in conductors  
*Phys. Review, Vol 32, pp 97-109, July 1928*

Thermal noise has a spectrum which, throughout the frequency range of interest in detector applications can be considered *white*, that is, frequency independent.

- o Any resistor at thermal equilibrium (no current flowing through it) exhibits only thermal noise
- o A metal film resistor features only thermal noise even when current flows through it
- o A non metallic resistor through which current flows, besides thermal noise may exhibit the so called *excess noise* whose spectrum has an  $f^{-1}$  frequency dependence.

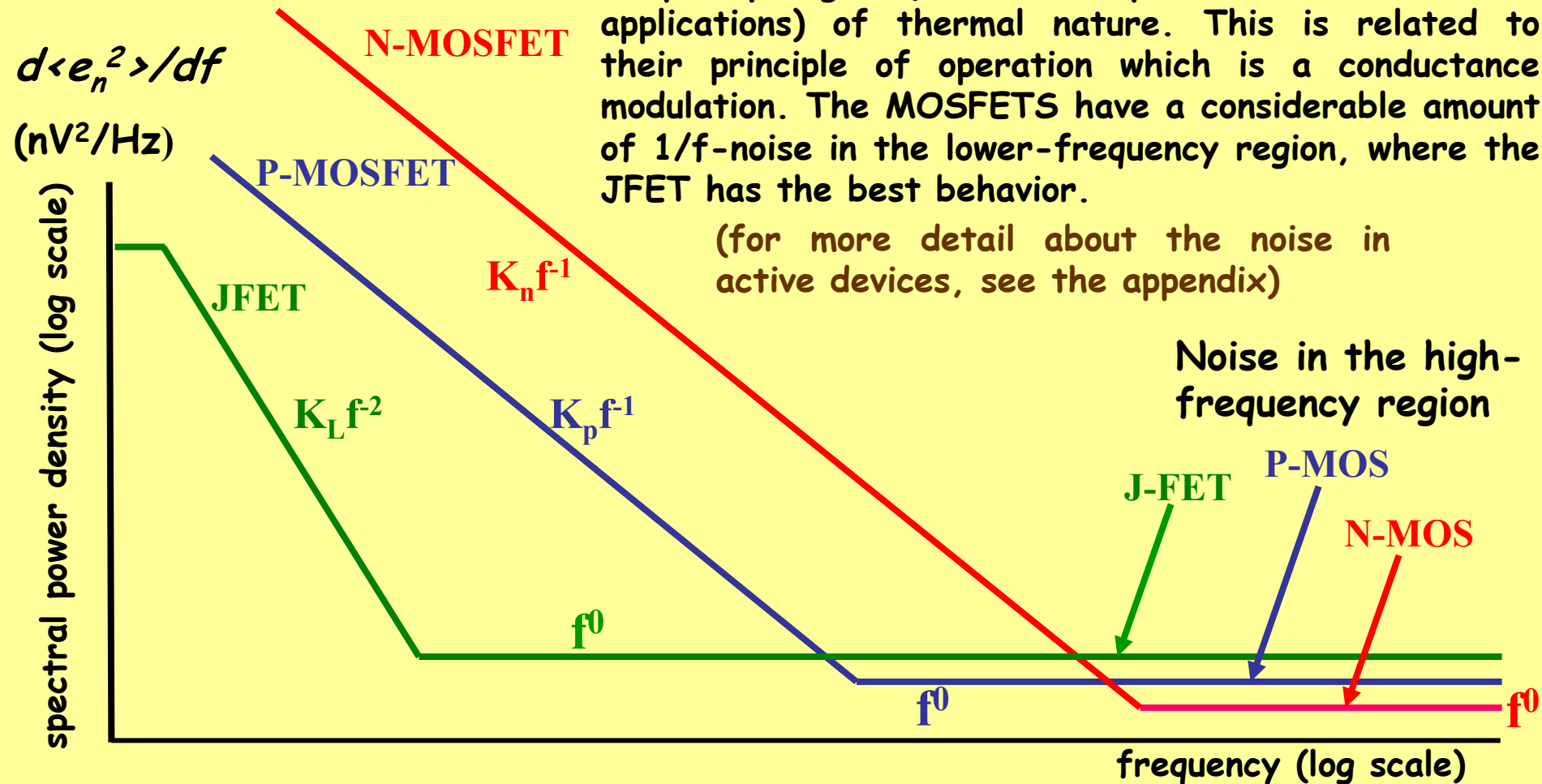
### Ideal capacitors are noiseless

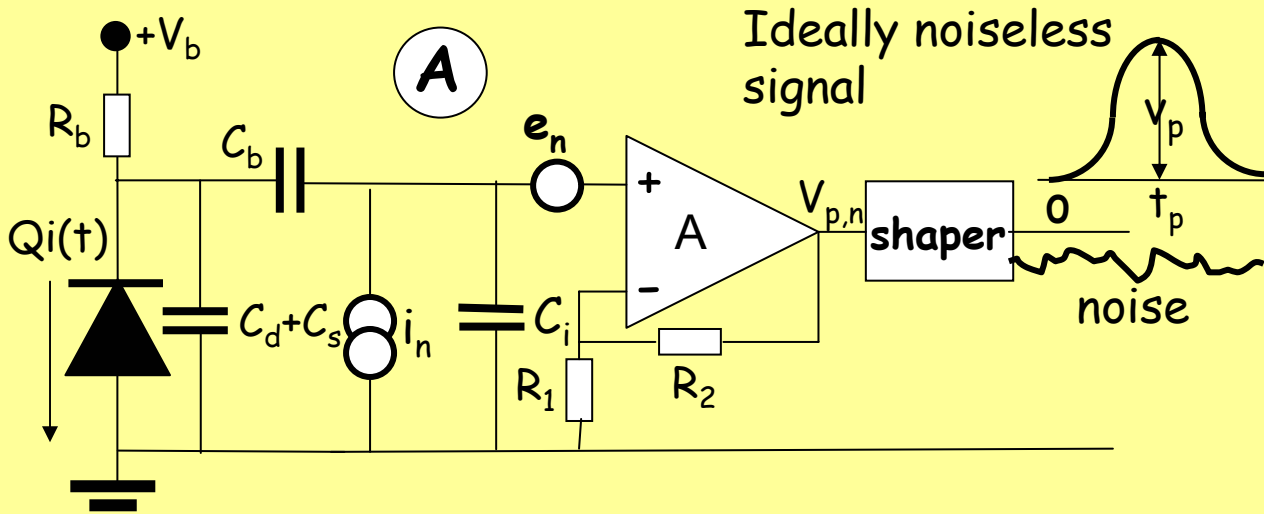
Real capacitors, instead, do feature noise associated with their dielectric losses. The spectral power density of dielectric has an  $f$ -type frequency dependence. Some specialists feel that in silicon-based X-ray spectrometers, that feature the highest achievable resolution, the ultimate limit is set by the dielectric noise in the detector itself.

**NOISE in ACTIVE DEVICES**- Qualitative comparison of the frequency dependence of the spectral power density  $d\langle e_n^2 \rangle/df$  in three active elements of different nature

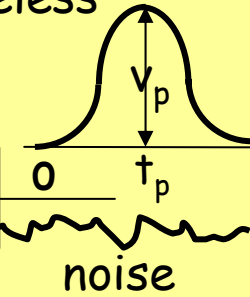
The three device feature a noise in the high-frequency region (the more important one in detector applications) of thermal nature. This is related to their principle of operation which is a conductance modulation. The MOSFETS have a considerable amount of  $1/f$ -noise in the lower-frequency region, where the JFET has the best behavior.

(for more detail about the noise in active devices, see the appendix)



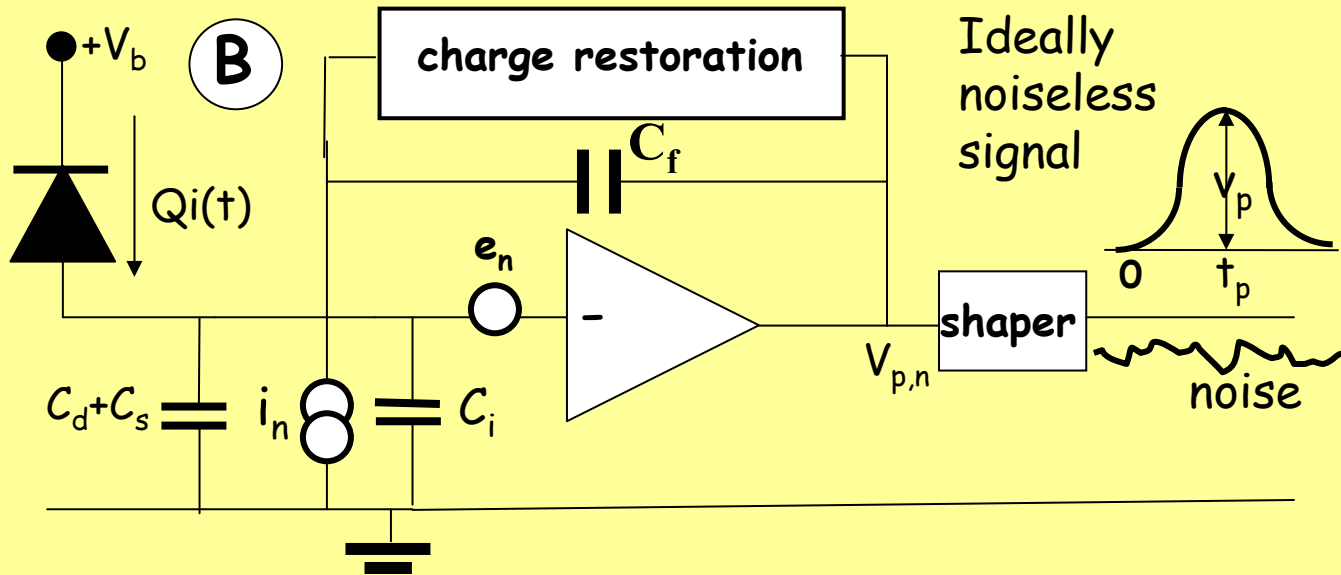


Ideally noiseless signal

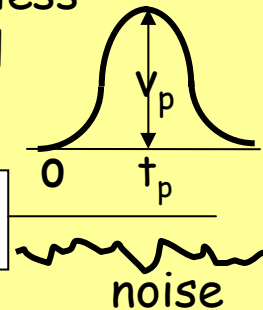


Direct integration of  $i(t)$  on the detector capacitance. The resulting voltage is amplified by a voltage-sensitive amplifier. Requires that the detector capacitance be reliable in value and stable. The detector is ac coupled to the preamplifier.

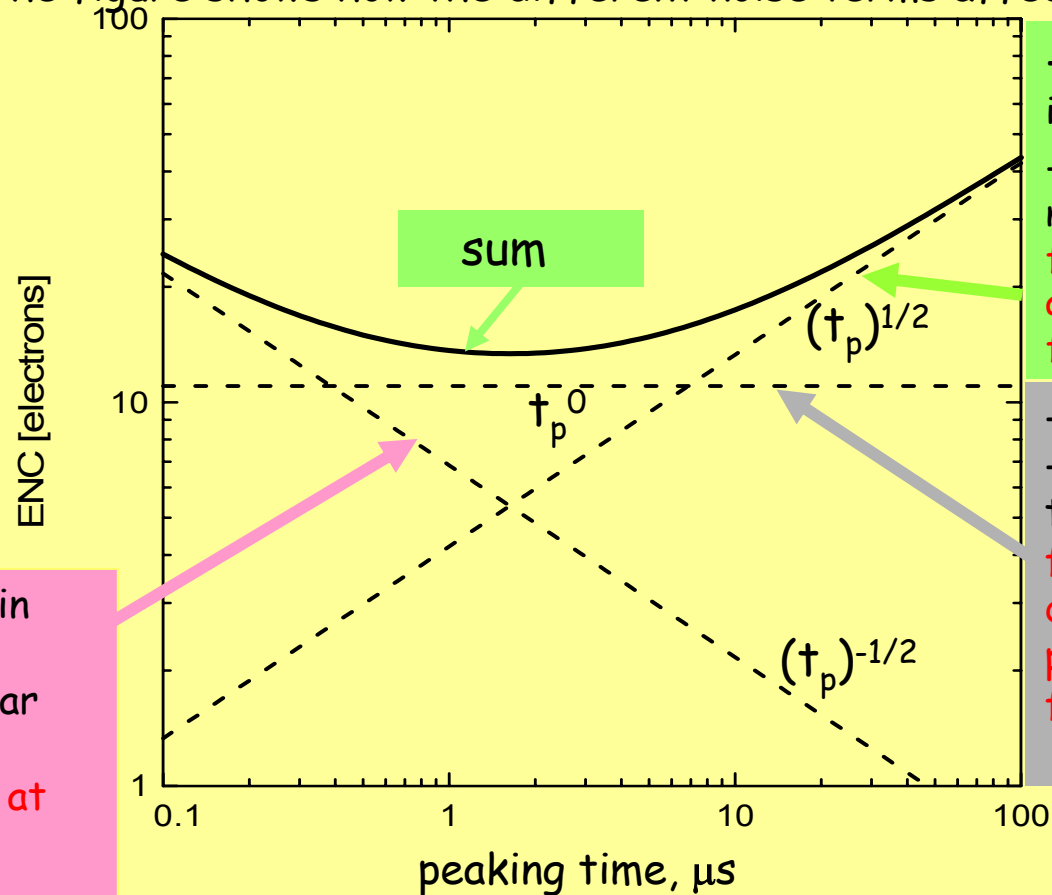
In this case the current integration takes place on the external capacitor  $C_f$ . This solution features also fewer sources of thermal noise than the previous one and this is the true reason why this is the best solution for the high resolution spectrometry.



Ideally noiseless signal



ENC is the value of the detector charge which carried by a  $\delta$ -impulse current  $i(t)$  produces at the shaper output a peak amplitude  $v_p$  of the ideally noiseless signal equal to the root mean square noise. The figure shows how the different noise terms affect ENC.



- white noise terms in  $i_n$   
 - channel lorentzian noise in JFETs:  
 frequency dependence at preamplifier output  $f^{-2}$

-channel  $1/f$ -noise  
 -dielectric noise term in  $i_n$  :  
 frequency dependence at preamplifier output  $f^{-1}$

-channel thermal noise in JFETs and MOSFETs  
 -collector noise in bipolar transistors:  
 frequency dependence at preamplifier output  $f^0$

Peaking-time dependence of the ENC contributions brought about by the spectral densities  $f^0$ ,  $f^{-1}$ ,  $f^{-2}$  in the noise at the preamplifier output.

## **APPLICATION-ORIENTED CHOICE of FRONT-END DEVICE**

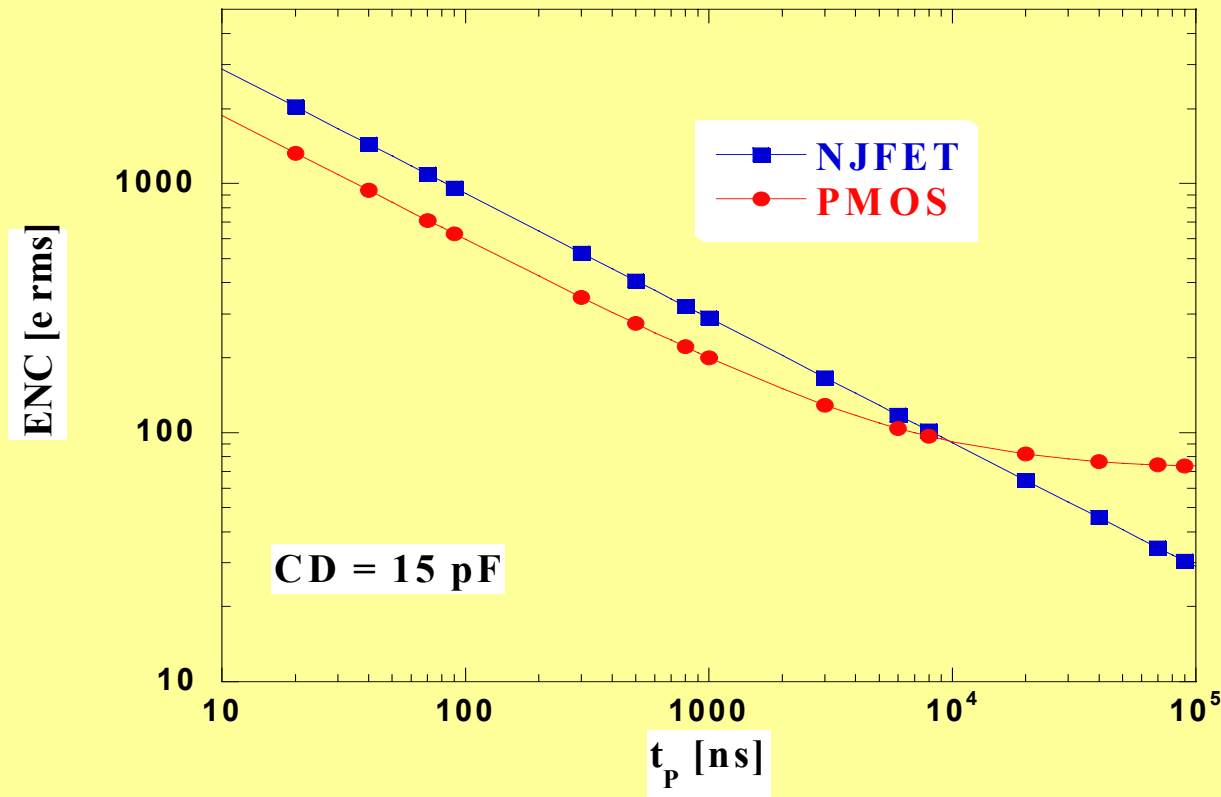
**Bipolar transistor** - Experiments featuring very high rates of events, requiring accordingly peaking times in the few-nanosecond region are the suitable domain of application for the bipolar transistor. At longer peaking times its base-current noise becomes a limitation

**Silicon junction field-effect transistor** - It is the choice front-end device for high resolution radiation spectrometry, especially for gamma and X-ray analysis with Ge and Si(Li) detectors. A problem, though, has to do with the fact that its minimum ENC occurs at the temperature of 140 K, which, if perfectly matches operation in LKr, would be unsuitable for a LAr calorimeter or for cooling by liquid N, the temperature at which Ge and Si(Li) detectors usually operate.

**Germanium junction field-effect transistor** - After some favor in the sixties as a low-noise device for cryogenic operation and then abandoned was resurrected a few years ago to cover the cryogenic region where silicon JFET fails.

**Enhancement-type MOSFET** - It has become the solution once the front-end design has moved to the monolithic implementation. This choice gained favor by virtue of the technological step called "device scaling" which consisted in a shrinking of gate length and a reduction in gate oxide thickness. Based on their noise features, P-channel is usually preferred to N-channel as a front-end device

ENC -  $t_p$  dependence of a JFET compared to the same dependence for a MOSFET. The comparison clearly shows the existence of a **noise floor** due to the  $1/f$ -noise in the MOSFET, which becomes cumbersome in the applications at long values of  $t_p$ .

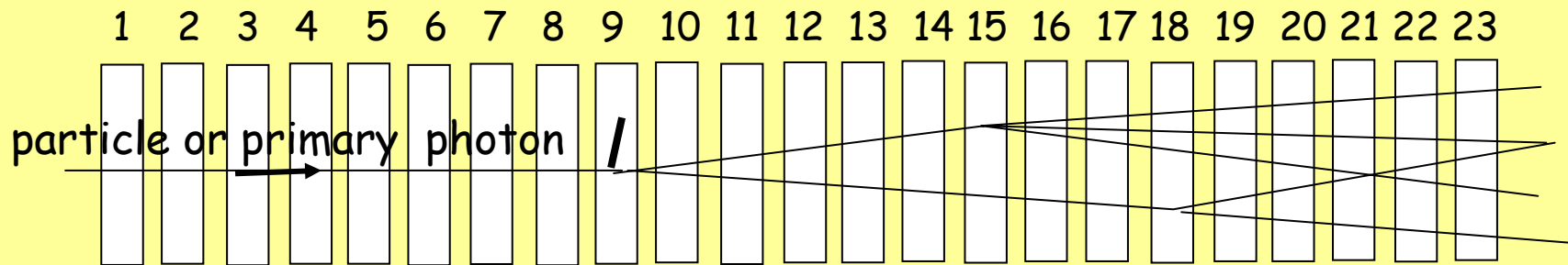


*The 1960-1970 decade was an important turning point for the energy-dispersive radiation analysis by virtue of the considerable advancement in detector technology and low-noise techniques.* Consider the following points.

- In the early sixties the best low-noise active devices were still considered the vacuum tubes. Theoretically the bipolar transistor was expected to provide nearly a factor for reduction in the spectral power density of high frequency noise, but this theoretical advantage was offset by its large noise in the base current.
- Gradually the advancement in JFET technology made them the most suitable devices in low-noise detector applications.
- The progress in Si and Ge refining techniques improved their quality, making them basic elements for the energy analysis of X and  $\gamma$  photons, thereby opening up a broad range of applications, like X-ray fluorescence, material analysis and so on.
- Such a high resolution spectrometry required more attention in identifying further sources of noise. *Dielectric noise in lossy capacitors was found as a potentially limiting term.*
- During this time span other sources of spectral line degradation were considered, in the attempt to extend the operation at high rates of events, which required a shorter  $t_p$  with effects on noise and ballistic deficiency and brought about the problem of baseline shift.
- Finally, as a **merit of Milan INFN**, Si detectors made their appearance in particle physics.

# ***Segmented detectors for position sensing***

Nowadays semiconductor position-sensitive detectors like highly segmented microstrip or pixel structures and vertex detectors based upon them have become essential parts of every experiment in physics and in several other fundamental sciences and applications. Before moving to them, it is worth describing a particular class of position-sensing detectors, the so called active targets that have been employed in some fixed-target experiments about two-to three decades ago. An active target is shown below.



The active target is a telescope of silicon detectors which implements a twofold function. Besides providing the target material it samples the specific energy loss  $dE/dx$  in the beam direction. The silicon active target of FRAMM experiment at CERN (late seventies-early eighties) employed 40 silicon layers.

The silicon telescopes brought about the noise limitations arising from the large detector capacitances, hundreds of pF, associated with the short values of  $t_p$  needed to comply with the high event rates during the accelerator spill. The optimization of the silicon active targets through three experiments was extremely instructive for the reasons listed below.

❖ In their first intervention (CERN SPS, 1968) it was noticed that they offered an interesting niche for the bipolar transistor as a front-end device and this is connected with **their comparatively small high-frequency noise at low currents.**

❖ Next came the remark that, being the detectors employed in the totally depleted mode, their association with a preamplifier featuring a *stabilized cold resistance* at the input, the time constant determined by the product of the detector capacitance and the cold resistance could be employed as a part of the shaping process. This solution was employed in the silicon active target of FRAMM experiment (CERN SPS, 1979-1983).

❖ The telescope-based active targets, better than perhaps other detector applications, underscored the limits set by the strict tie between sensitive area and detector capacitance and therefore, noise. Likely, active targets contributed to focus the attention of Emilio Gatti, who had taken an active part in their operation, on possible ways of removing such a tie. The result was the invention of the Silicon Drift Chamber by E. Gatti and P. Rehak, a very smart solution to the problem.

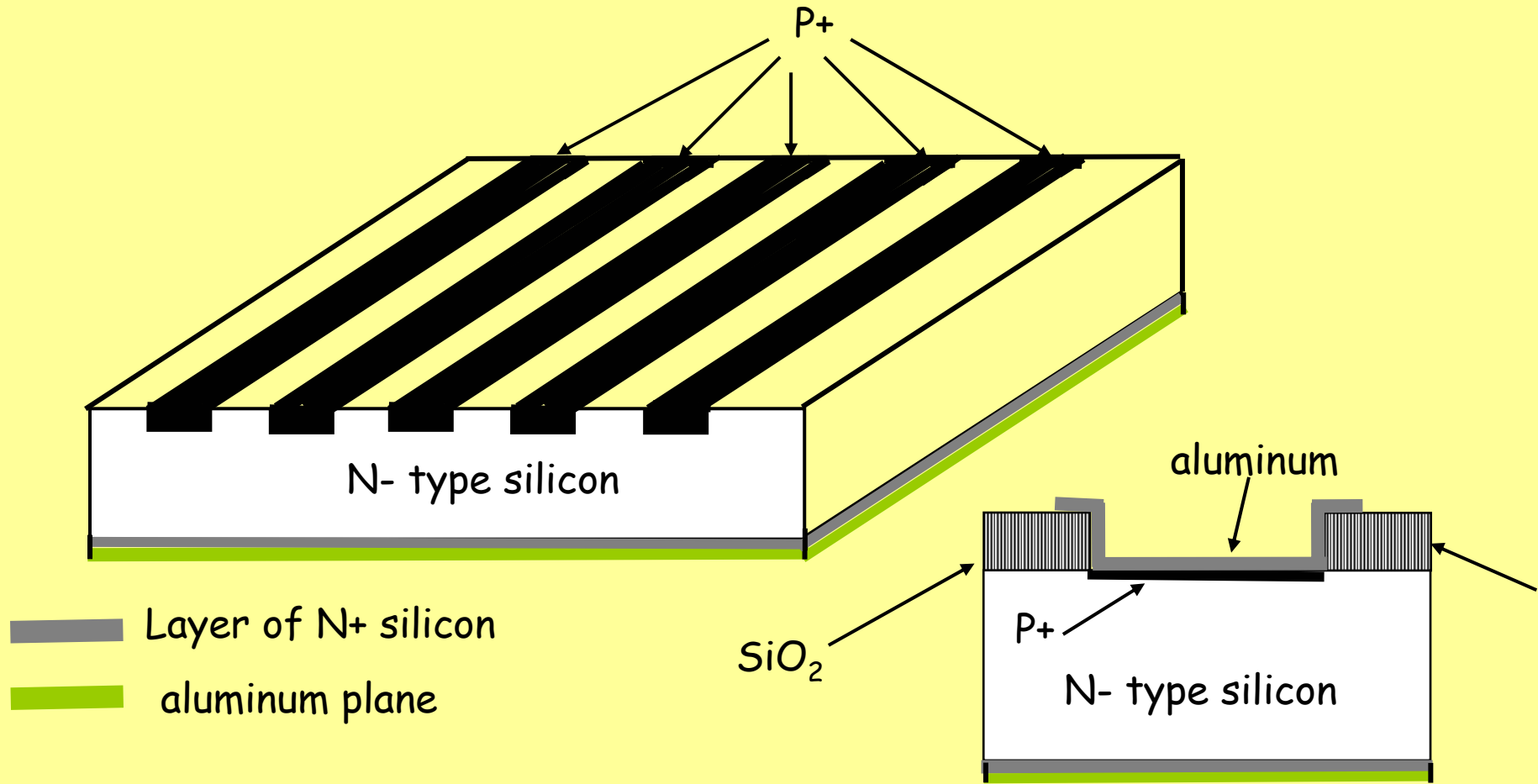
The first microstrip vertex detector was installed in the E687 fixed-target experiment at FERMILAB in 1985.

At about the same time vertex detectors were installed in Delphi and Aleph collider experiments at LEP.

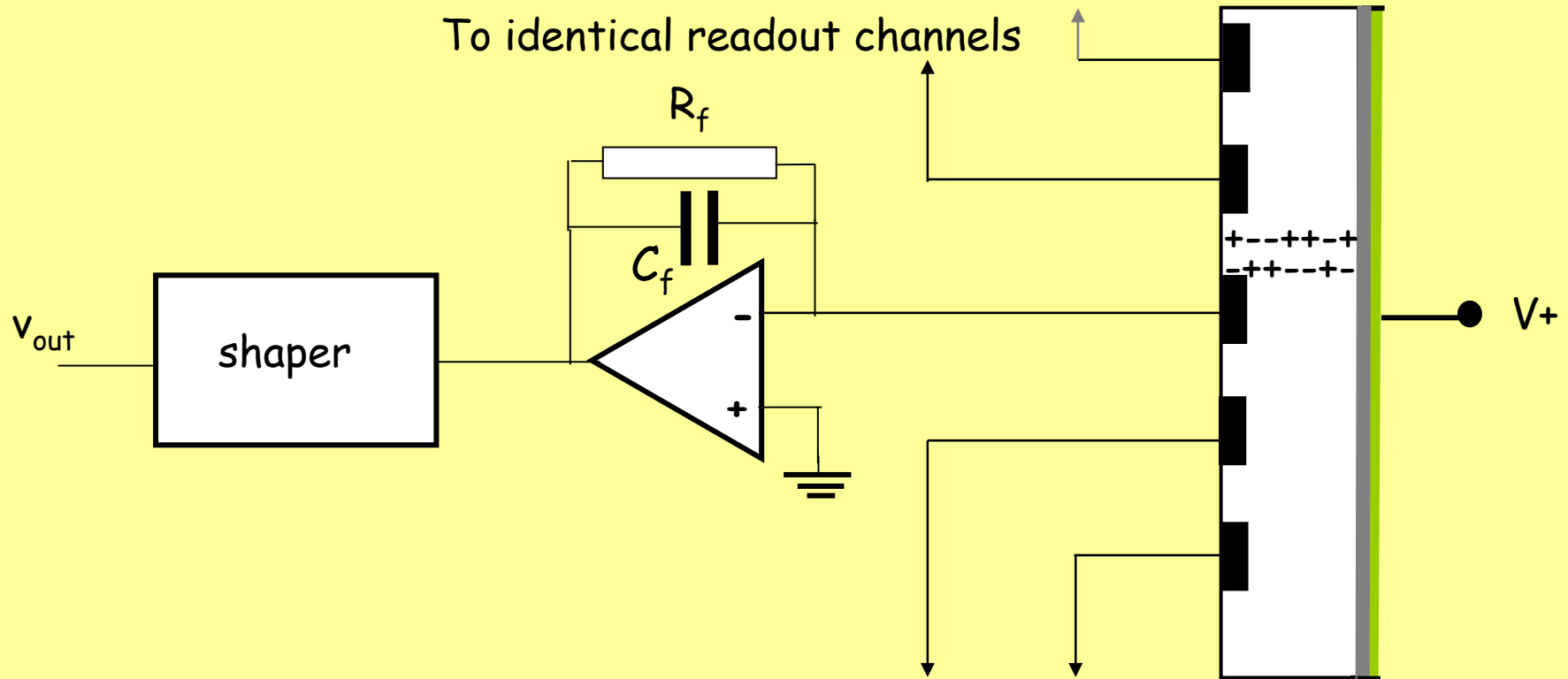
Since then, many more microstrip vertex detectors have been introduced in particle physics (CLEO, CDF, D0, BaBar). Much more complex vertex detectors employing both microstrip and pixel structures have been developed for the forthcoming experiments at LHC.

Just one example to point out the importance of vertex detectors: at **CDF the vertex detector**, which was introduced when the experiment was already advanced, **was instrumental in the detection of the TOP QUARK**

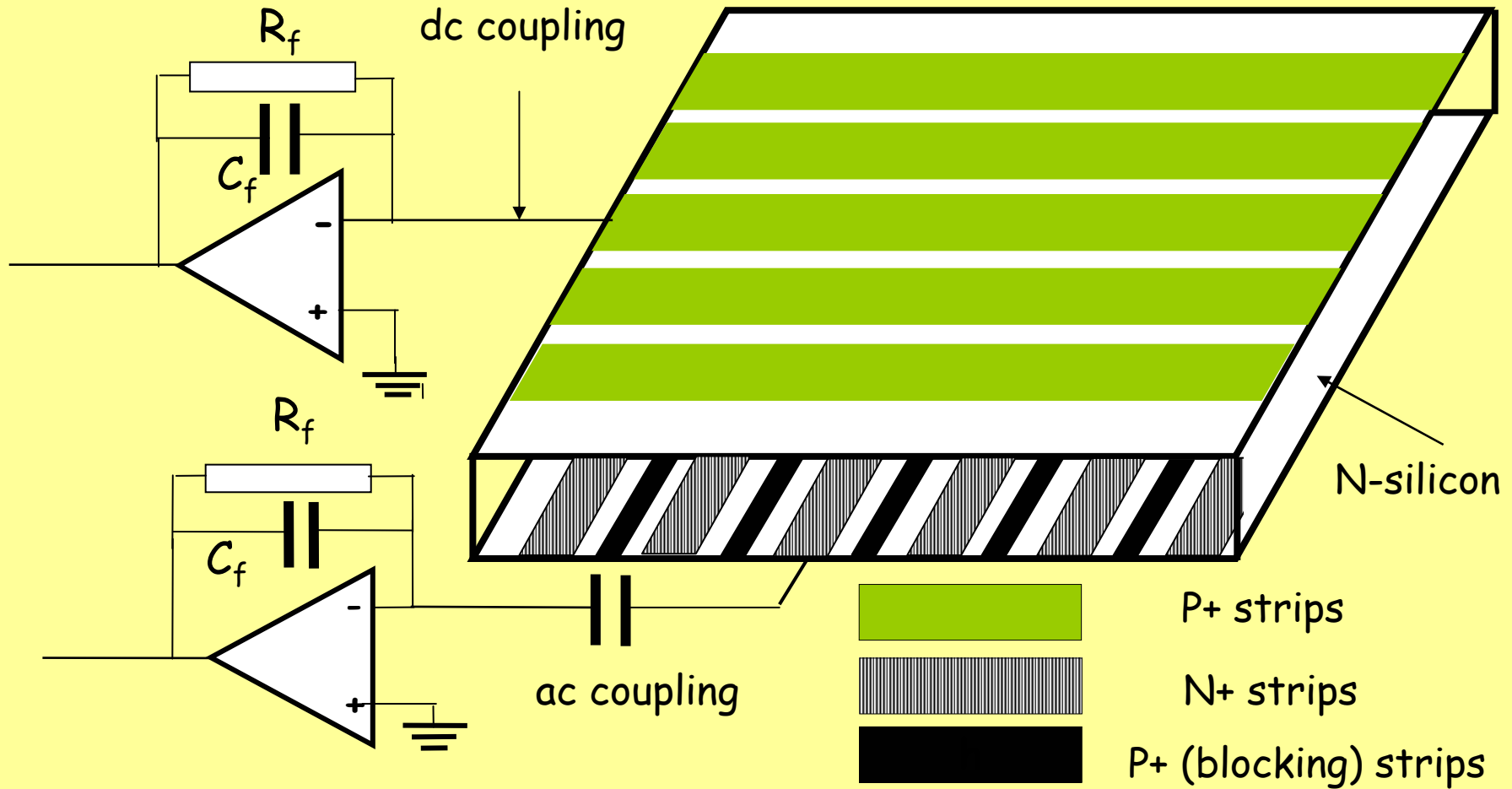
## A SINGLE-SIDED MICROSTRIP DETECTOR



## JUNCTION-SIDE ( P+STRIPS ) READOUT OF A SINGLE-SIDED MICROSTRIP DETECTOR

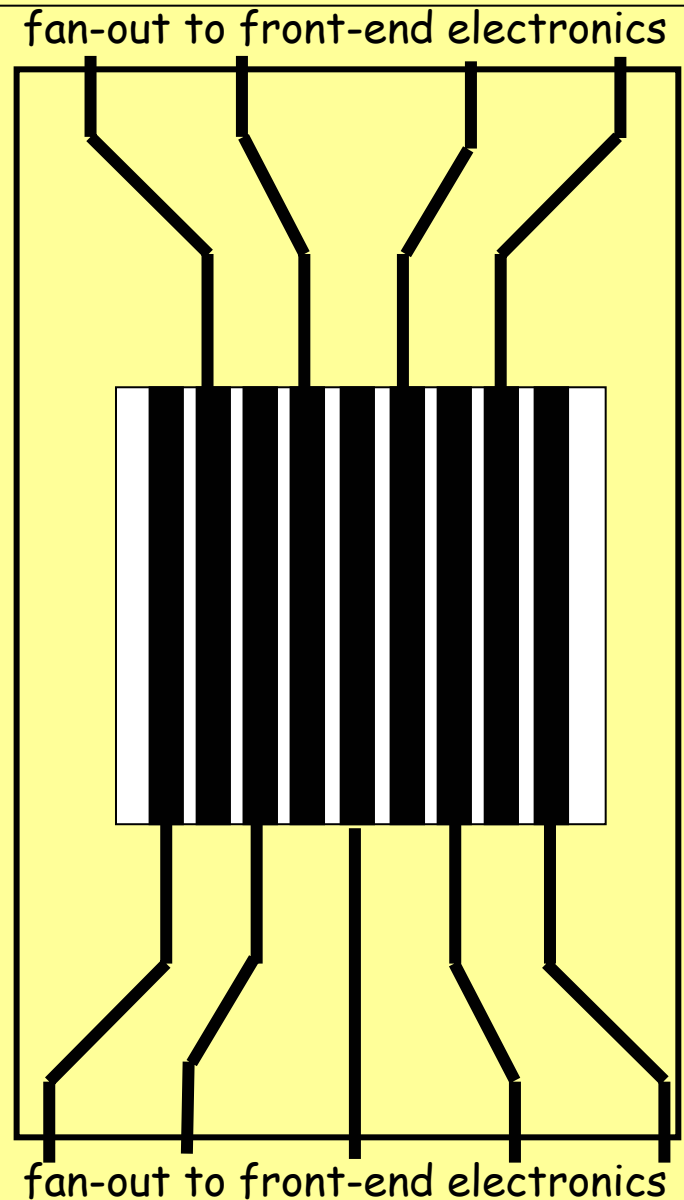


Double-sided microstrip detector. The readout preamplifiers are dc coupled on the junction side and ac coupled on the ohmic side.

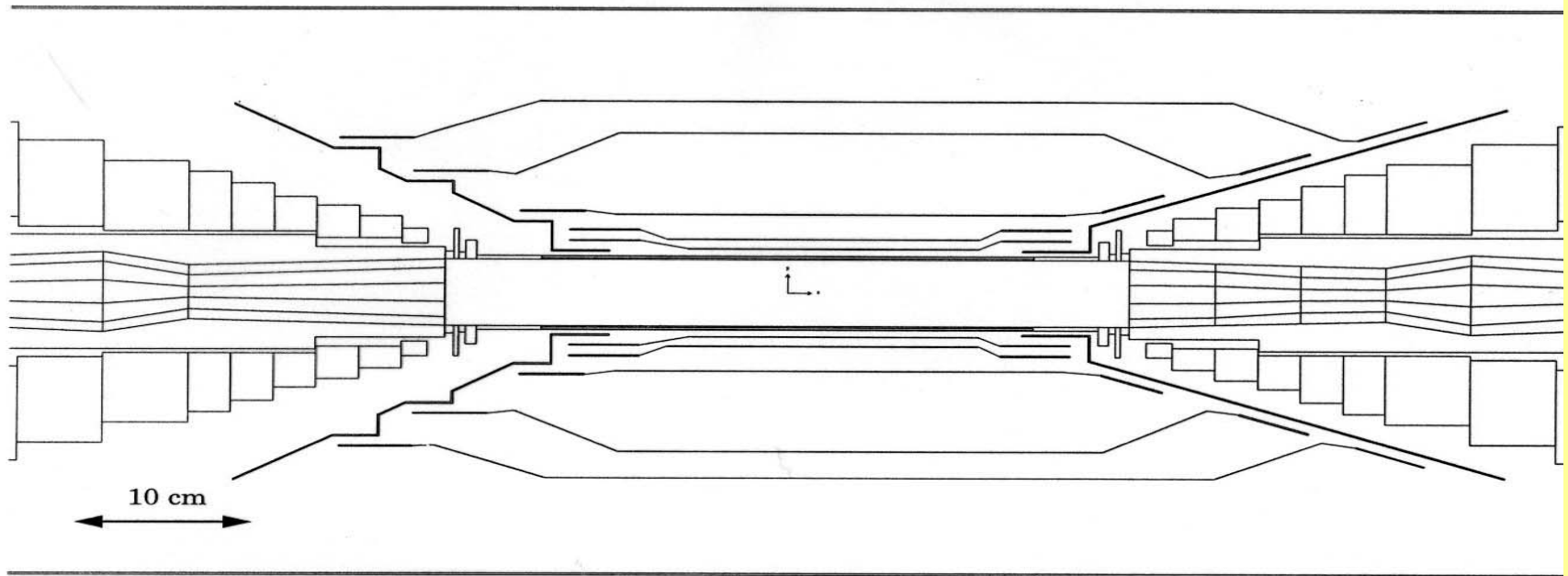


The first microstrip vertex detector to come into use was probably the one developed by Milan and installed in 1985 in the E687 fixed-target experiment on the wideband photon beam at Fermilab. The fixed-target nature of the experiment allowed the signal coupling to the front-end electronics through a printed board fan-out. This left full freedom in the choice of the front-end device for the best noise characteristics. For instance, in E687 the preamplifiers were thick film circuits employing at the input a depletion-type mosfet of good noise features. The freedom in the choice of the input device was, however partially offset by the additional capacitance introduced by the fan-out.

When experiments changed from fixed target to colliding beams the geometry of the vertex detector changed. The microstrip layers are arranged in a cylindrical geometry. Besides, vertex detectors of higher complexity were required. It became impossible to send out every microstrip signal along an individual lead. Multiplexing features were needed to reduce the number of outgoing cables. Therefore, monolithic front-end implementation became essential as it happened for Delphi and Aleph experiments at LEP.



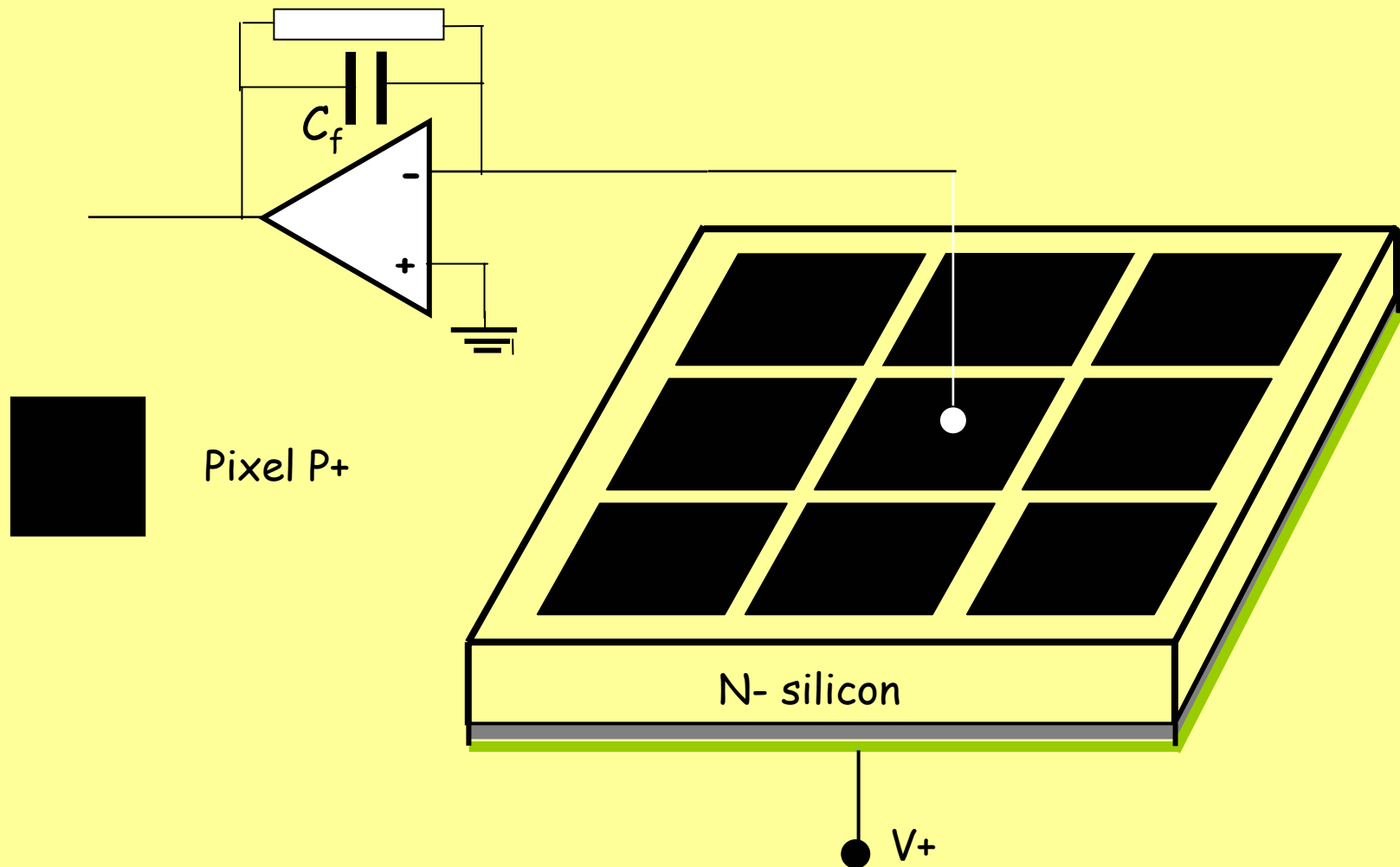
**Cross-Section of the SVT**



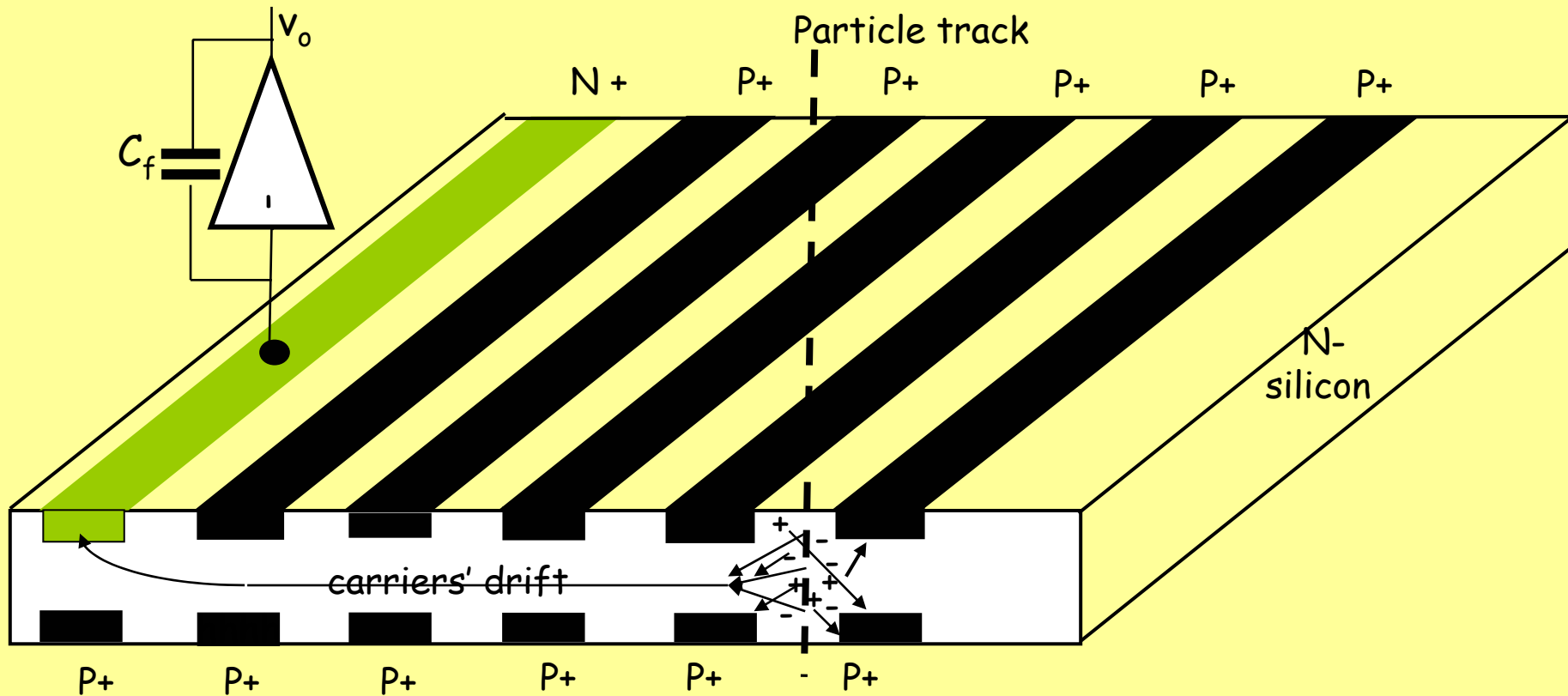
- 5 layers inside a support tube of radius 20 cm
- 1 m<sup>2</sup> of double-sided ac-coupled silicon strip detectors
- 150,000 readout channels (outside the active volume)
- 2 Mrad of radiation tolerance in the electronics (worst case)

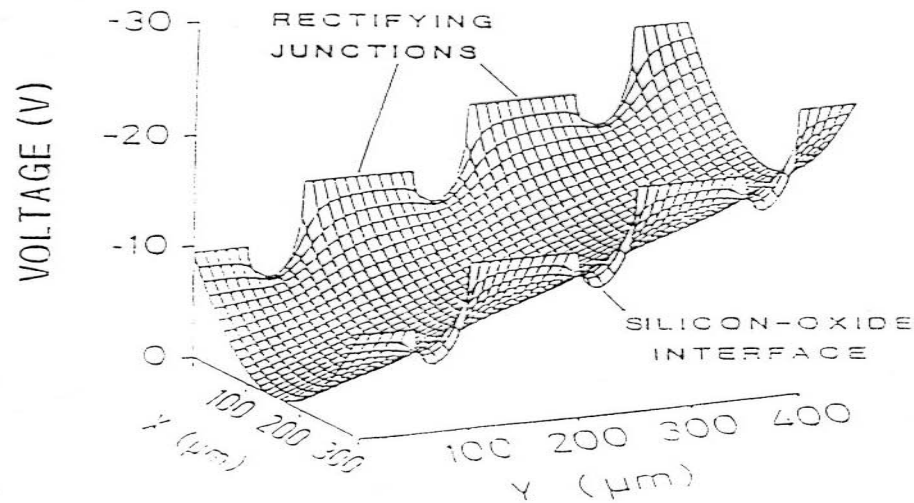
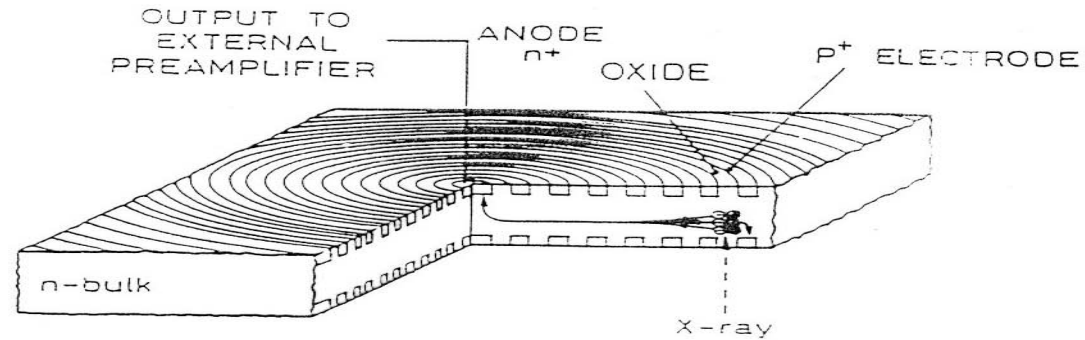
Section of the Silicon Vertex Tracker of BaBar experiment at SLAC e+e- collider

## A PIXEL DETECTOR



**THE DRIFT CHAMBER** - The drift chamber invented by E. Gatti and P. Rehak employs an original charge transport method. The capacitance presented to the readout preamplifier by the collecting electrode is largely independent of the sensitive area. This feature reduces the effect of preamplifier noise to a remarkable extent.





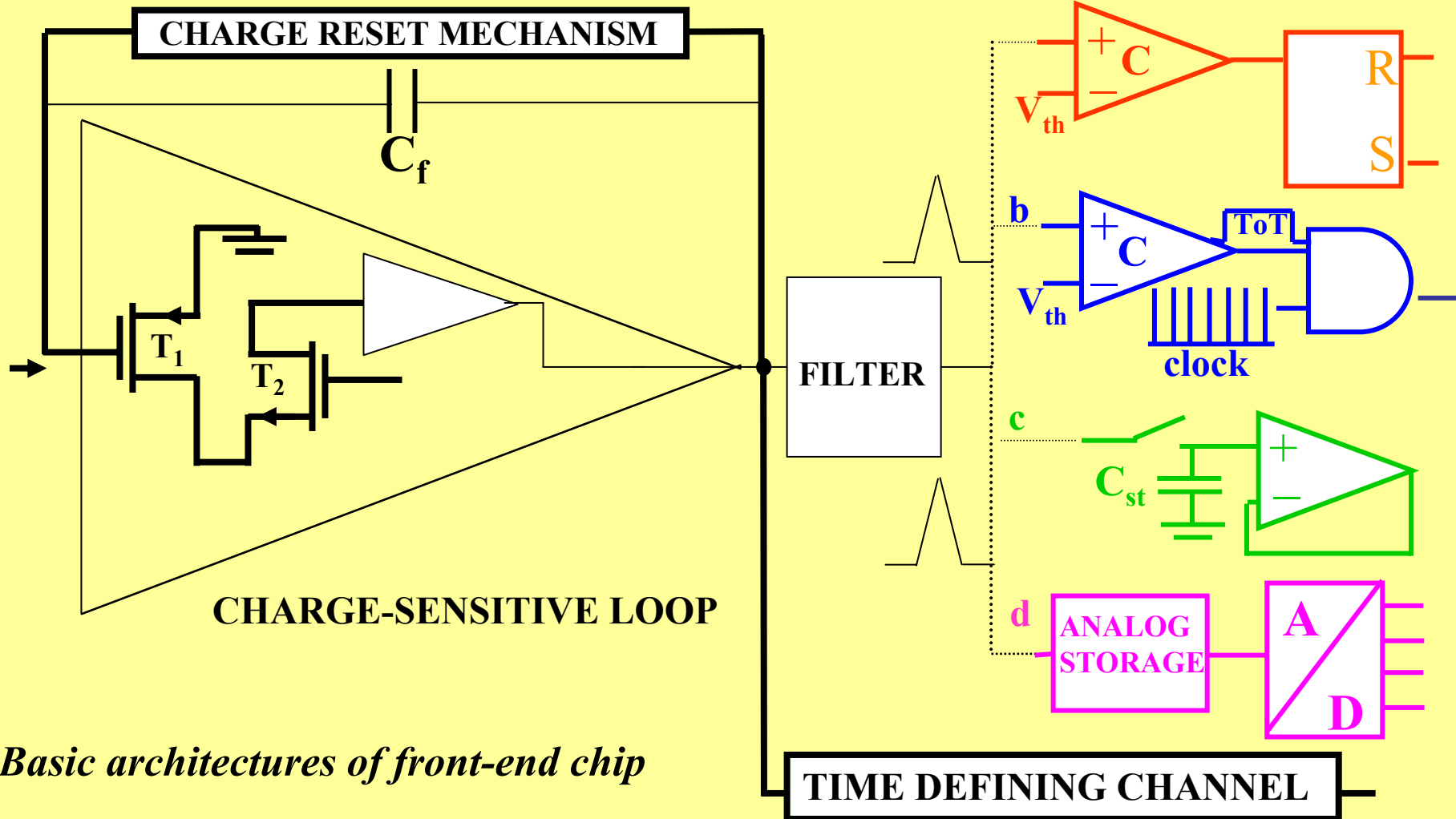
The introduction of microstrip and pixel detectors in collider experiments urged a thorough reconsideration of the front-end concepts. Let's review it here. As already pointed out, a monolithic front-end design appeared to be the only viable solution at the time of the LEP-oriented R&D activities in the early eighties. At the onset of the data taking, Aleph and Delphi experiments were equipped with monolithic front-end systems for the readout of their vertex detectors. The approach followed was based upon CMOS processes.

The CMOS processes at that time featured a comparatively long gate, 4 to 5 microns, which resulted in rather large channel thermal noise and a thick gate oxide, some tens of nanometer. This was responsible for a large 1/f-noise and for its sensitivity to the absorbed radiation. With the aim of reducing the 1/f-noise and the radiation sensitivity the attention turned to monolithic processes featuring a JFET compatible with the CMOS process. Front-end systems were realized employing for instance

- o the Fraunhofer Gesellschaft process P and N channel JFETs along with CMOS
- o the DMILL process, P-channel JFET, NPN bipolar transistors along with CMOS

Effort in this direction was certainly fruitful until the device scaling offered CMOS processes with a gate length in the submicron and then in the deep submicron region, down to less than 100 nanometers and gate-oxide thickness of a few nanometer.. The results were a reduction of channel thermal noise and 1/f-noise, along with an improved radiation resistance.

A more significant advancement in the front-end conception was required by the silicon drift detector. To retain the remarkable feature of a capacitance in the 100 fF region the front-end elements were realized on the detector-grade silicon where the detector itself resides.



*Basic architectures of front-end chip*

***Back to the origin or no detector  
ever becomes obsolete***

## THE LHC LUMINOSITY MONITOR

### THE CONCEPT WHICH UNDERLIES THE LUMINOSITY MONITOR FOR LHC

Proton-proton collisions at the Interaction Points (IP) of (LHC) will produce high fluxes of neutrons and photons that will be intercepted by the neutral absorbers located about 140m downstream the IP1 and IP5 collision points. *The energy associated with the showers initiated by the neutral flux from the IPs is proportional to the charge of the colliding bunches and hence to the luminosity.*

The study was focused on a detector able to provide information on the shower population with response times compatible with the 40 MHz bunch collision frequency. The idea was to install it into a slot machined inside the copper core of the absorbers in order to monitor and optimize the LHC luminosity in a bunch-by-bunch operation.

The first problem was identifying the detector type suitable for the purpose. The luminosity monitor is a nearly zero-angle detector and as such it will be exposed to an extremely high dose of radiation. It should stand, before a replacement is possible, up to 1 G Gy, a dose exceeding by at least two orders of magnitude that expected for detectors in LHC experiments. Ordinary solid-state detectors were discarded as it was concluded that they wouldn't survive long enough for the purpose. Polycrystalline CdTe was proven to be promising, but later it was abandoned because of technological difficulties in the realization of adequately large sensitive areas. The best solution was identified to be a multigap ionization chamber operating at a high pressure of the filling gas.

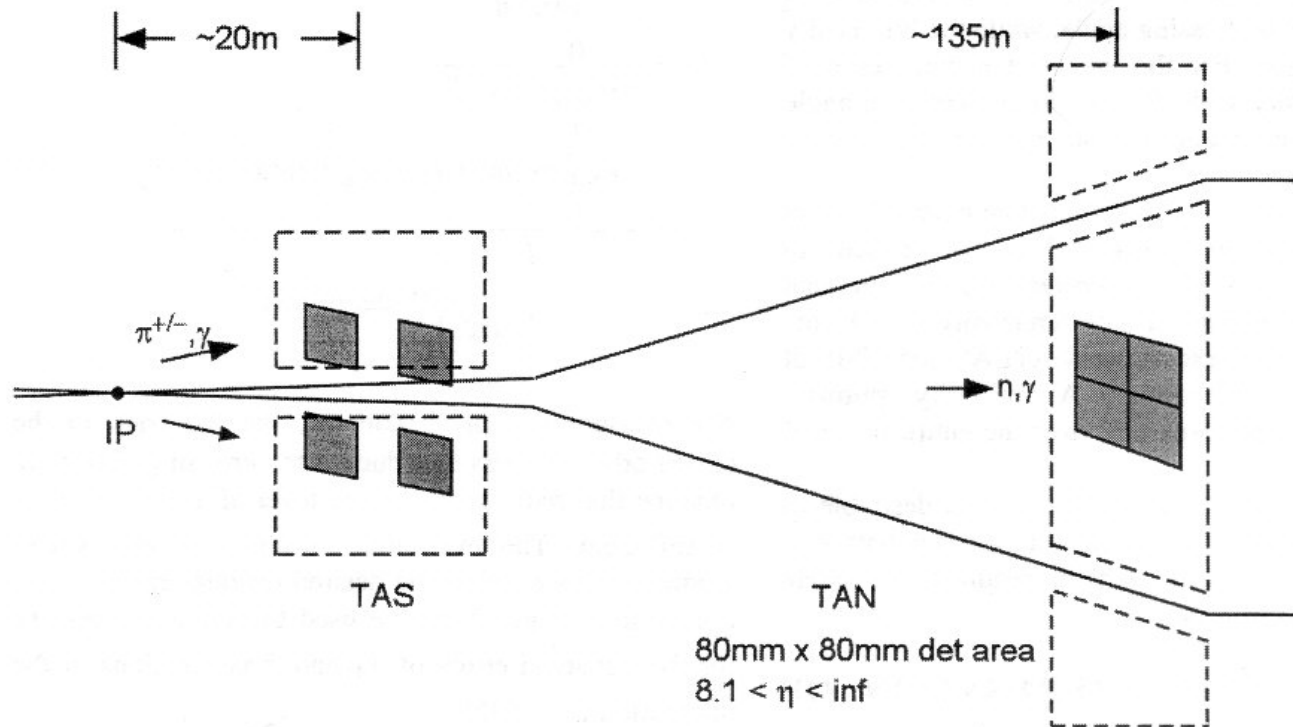


Fig. 4: Illustration of ionization chamber detectors in the TAN and TAS absorbers.

Questions:

❖ How can a gas filled ionization chamber lead to a sufficient energy loss by minimum ionizing particles?

This problem was addressed by adopting for the chamber a multigap structure and operating it at a high gas pressure

❖ How can an ionization chamber operate at a 40 MHz repetition rate while it is known that the drift velocity of electrons in a gas is low?

This problems was addressed by designing thin gaps to reduce the distance traveled by the electrons and by using a mixture (Ar+N<sub>2</sub>) which features a higher electron drift velocity than pure Ar. Addition of organic molecules, which would further increase the electron drift velocity was avoided on the basis of considerations of radiation hardness.

❖ What measures were taken to make such a detector to meet the radiation hardness specifications?

One is the use of filling gases of strictly inorganic nature (Argon and Nitrogen),  
The second one is the continuous fluxing of the gas mixture, in order to make sure that the damaged filling mixture is continuously removed.

# DETECTOR EVOLUTION

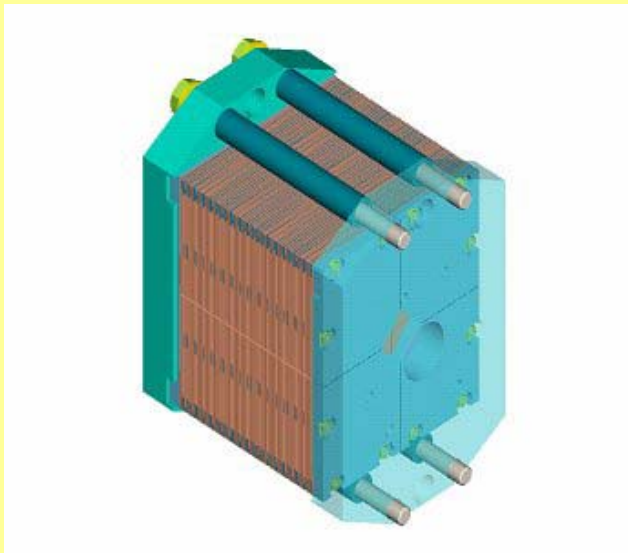
## First version (years 2000, 2001)

$$N_{\text{GAP}} = N_{\text{SER}} \times N_{\text{PAR}} = 60$$

$$x_{\text{GAP}} = 0.5 \text{ mm}$$

$$\text{drift vel.} = 3 \text{ cm}/\mu\text{s} \text{ (98\% Ar + 2\% N}_2\text{)}$$

$$C_{\text{DETECTOR}} = C_{\text{GAP}} \times N_{\text{PAR}} / N_{\text{SER}}$$



## Second version (years 2003 e 2004)

$$N_{\text{GAP}} = N_{\text{PAR}} = 6$$

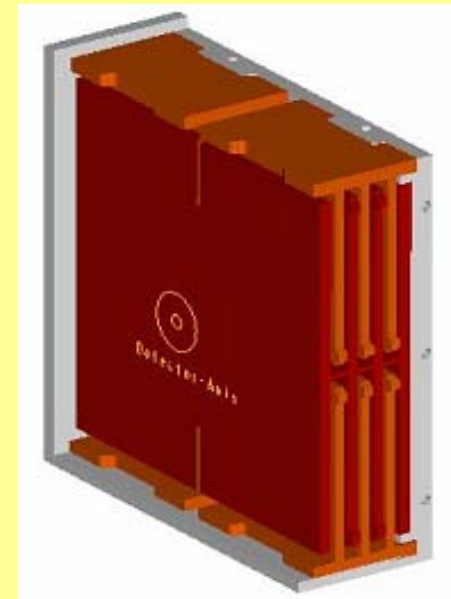
$$x_{\text{GAP}} = 1 \text{ mm}$$

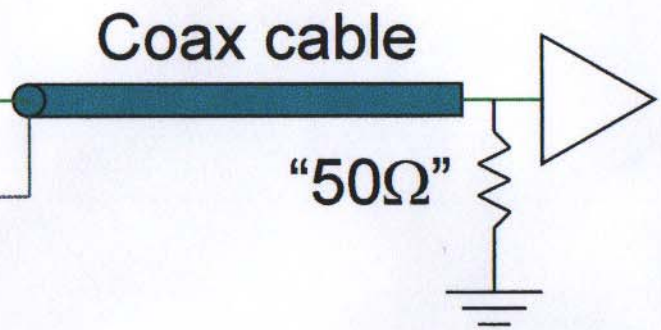
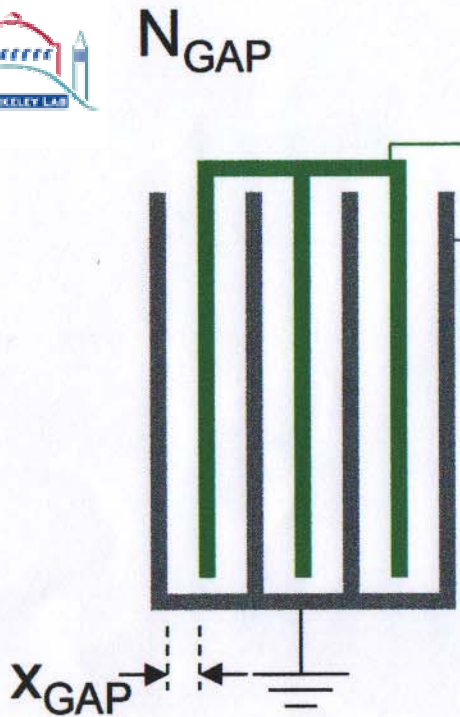
$$\text{drift vel.} = 4.5 \text{ cm}/\mu\text{s} \text{ (94\% Ar + 6\% N}_2\text{)}$$

$$Q_{\text{GAP}} \text{ doubled}$$

$$C_{\text{GAP}} \text{ halved}$$

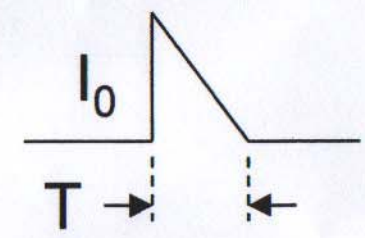
$$C_{\text{DETECTOR}} = C_{\text{GAP}} \times N_{\text{PAR}}$$





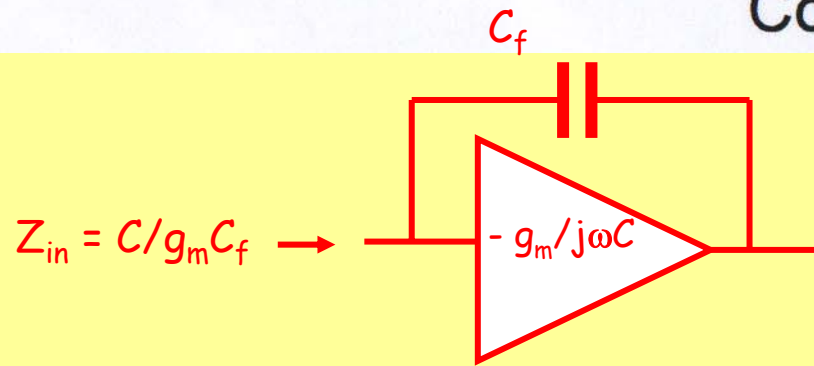
In reality the "50 Ω" termination, for low-noise operation, has been realized with the cold-resistance approach shown in red at the bottom of the page.

Ionization Current



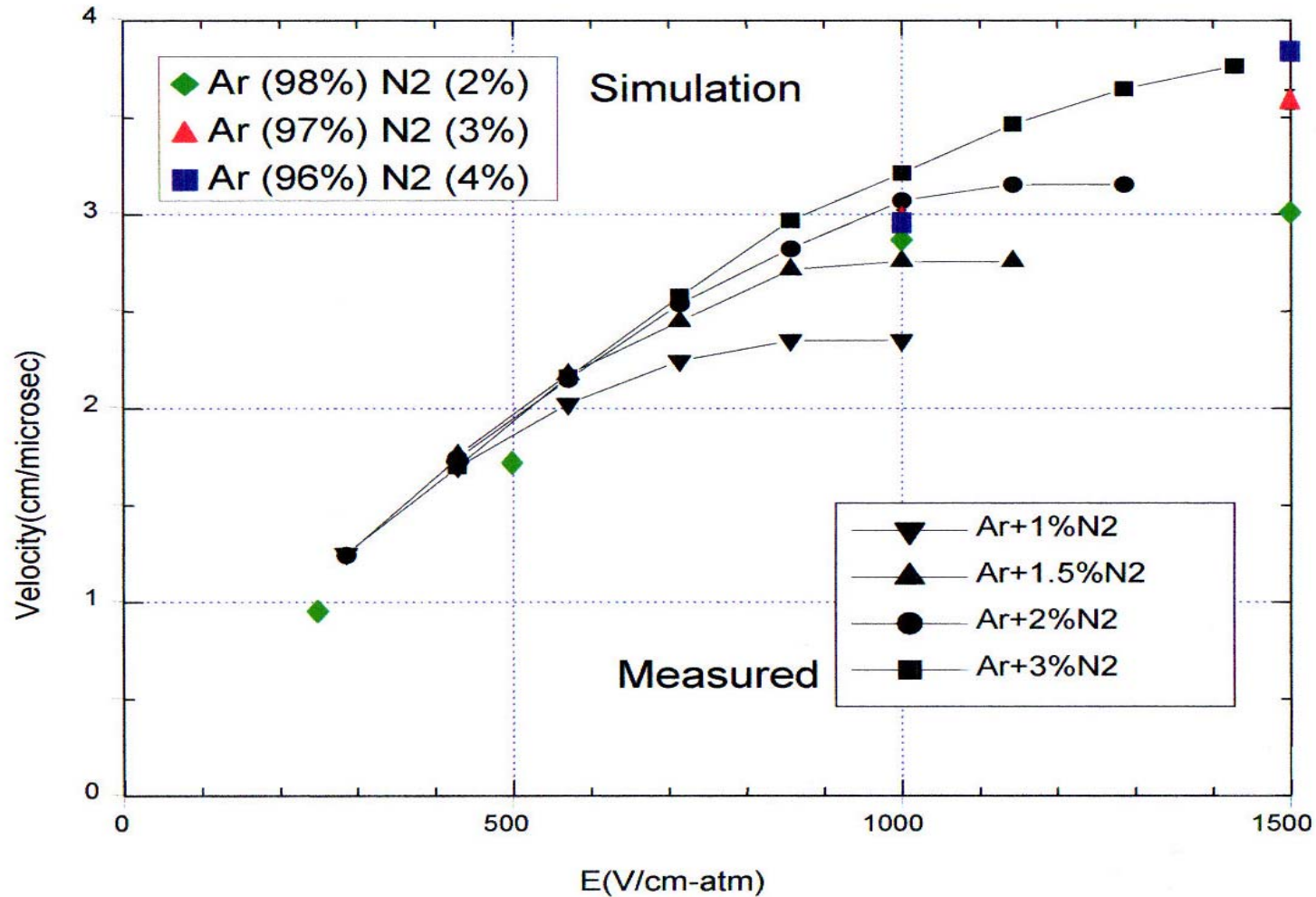
Time Constant

$$50\Omega \times C_{\text{DETECTOR}}$$



$g_m$  is the transconductance of the active block and  $C$  in the bandwidth-limiting capacitance

## Drift Velocity



## C O N C L U S I O N S

The anticipated task of this talk was revisiting the importance that ionization-based detectors had from a twofold point of view. One was the remarkable contribution they gave to the advancement of physics. The second one was the fallout which resulted in the knowledge of detector and front-end operation and more generally in the evolution of the measurement techniques. Nowadays radiation-based detectors are of a fundamental importance in pure and applied sciences and they benefit of the effort produced by a six decade activity of a number of scientists and technologists worldwide.

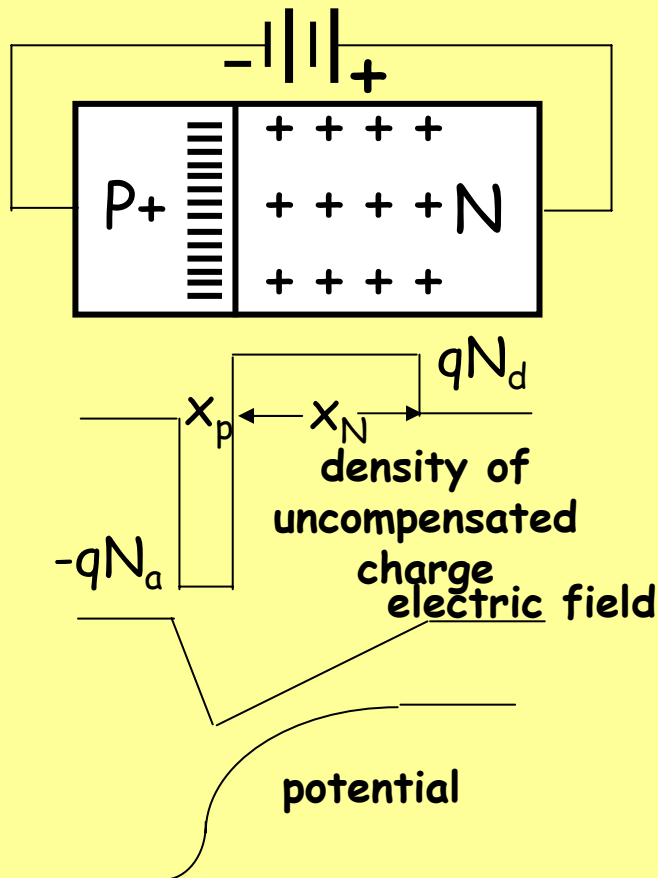






# **Appendix**

# ***Semiconductor detectors***



**P+region:** trivalent impurities (B) with density  $N_a$  - free carriers holes(+), ionized atoms with negative charge

**N region:** pentavalent impurities (As) with density  $N_d$ , free carriers electrons (-), ionized atoms with negative charge

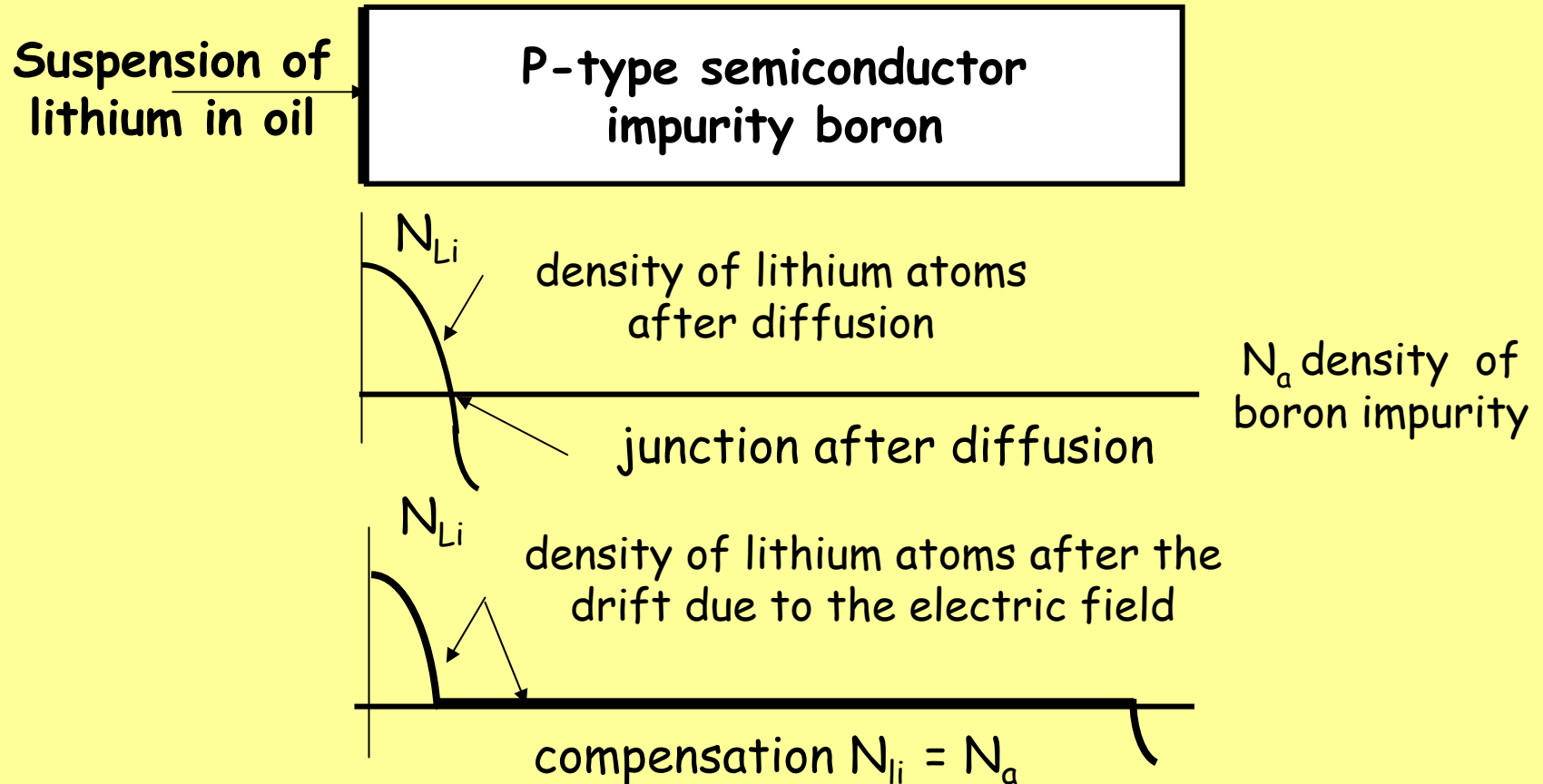
**Charge balance:**  $x_p N_a = x_N N_d$  which shows that the space charge region extends more deeply into the region of lower impurity density.

**Case of  $N_a \gg N_d$ ,** the depleted region extends almost entirely in the N region,  $x_p \ll x_N$  and  $x_N$  is proportional to  $(V/N_d)^{1/2}$

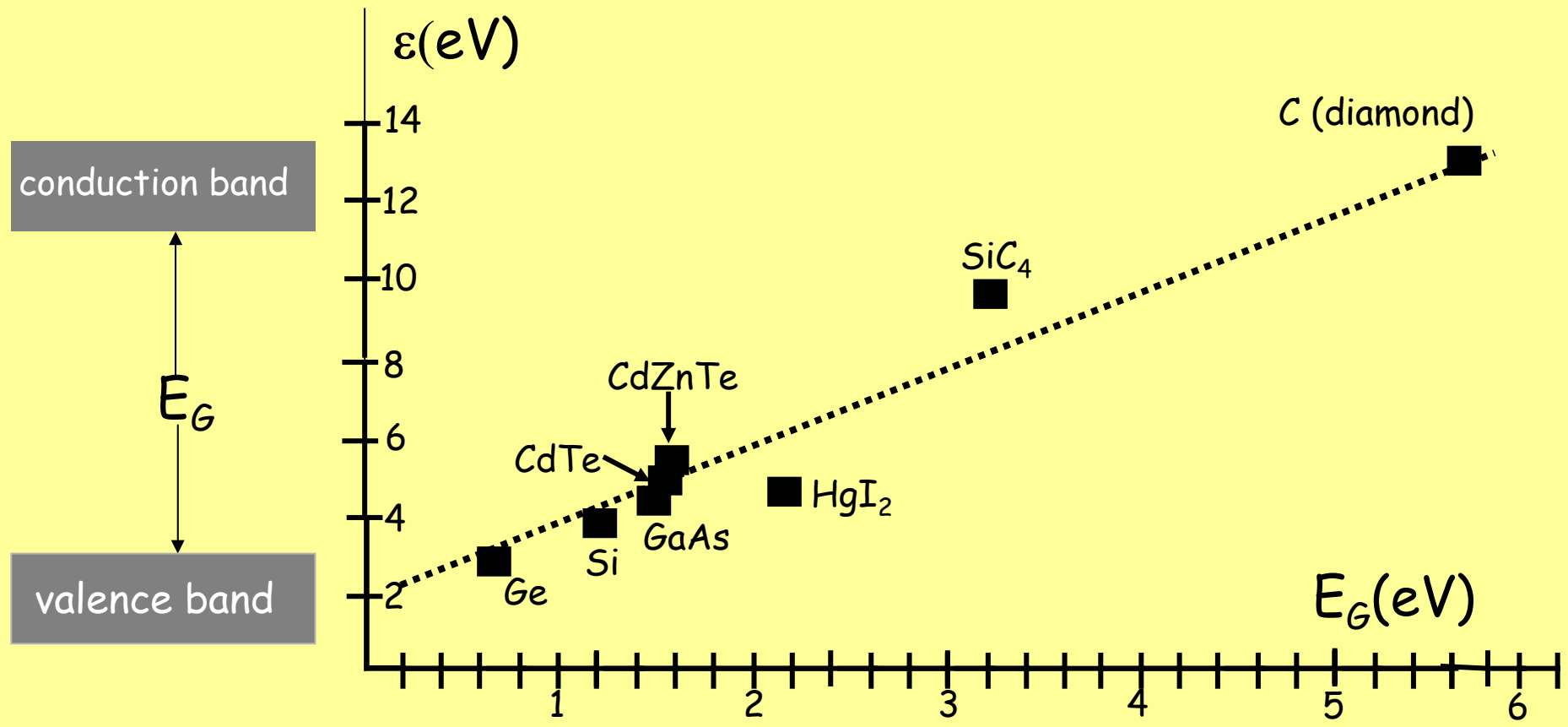
In the real implementation of Si detectors the **P+ region is much thinner and much more heavily doped as compared to the N region .**

The size of the very lightly doped N region, defines the sensitive thickness of the detector. For the sake of making the explanation easier, the figure does not respect the actual scales of thicknesses and doping levels of P and N regions. **With some semiconductors, instead of a classical P-N junction, a Schottky barrier is adopted.**

**THE PROCESS OF LITHIUM DRIFT IN SILICON IS USED TO OBTAIN LARGE THICKNESSES OF A NEARLY INTRINSIC MATERIAL**



Relationship between the energy gap  $E_G$  and the value of  $\epsilon$ , the energy required to create an electron-hole pair in some materials commonly employed in the realization of solid-state detectors.



**CHARACTERISTICS OF THE MATERIALS MORE COMMONLY USED  
IN THE REALIZATION OF SOLID STATE DETECTORS**

MATERIAL	$E_G$ (eV)	$\mu_e$ (cm <sup>2</sup> /Vxs)	$\mu_h$ (cm <sup>2</sup> /Vxs)
Ge	0.72	3900	1900
Si	1.13	1400	480
GaAs	1.43	8000	400
CdTe	1.44	1100	100
CdZnTe	1.5 - 2.2	1350	120
CdSe	1.73	720	75
HgI <sub>2</sub>	2.13	100	4
C	5.4	2200	1600
SiC <sub>4</sub>	3.2	1000	115

$\mu_e$  electron mobility                       $\mu_h$  hole mobility

**At the temperature of 77 K the mobilities of Ge and Si are higher.**

Ge:  $\mu_e = 3.6 \times 10^4$  cm<sup>2</sup>/Vxs     $\mu_h = 4.2 \times 10^4$  cm<sup>2</sup>/Vxs

Si:  $\mu_e = 2.3 \times 10^4$  cm<sup>2</sup>/Vxs     $\mu_h = 1.1 \times 10^4$  cm<sup>2</sup>/Vxs

# ***NOISE***

Once skilled shielding and grounding techniques have eliminated all removable disturbances that the surrounding environment induces onto the detector system, the fundamental noise associated with the detector and the electron devices in the front-end system remains as a limitation. The noise of this nature falls into the category of stochastic process  $[N(t), t]$ . It will be assumed that the conditions required for the existence of the spectral power density of the process,  $S(f)$ , are met. The meaning of  $S(f)$  is defined by the following relationship:

$$d\langle N^2 \rangle / df = S(f)$$

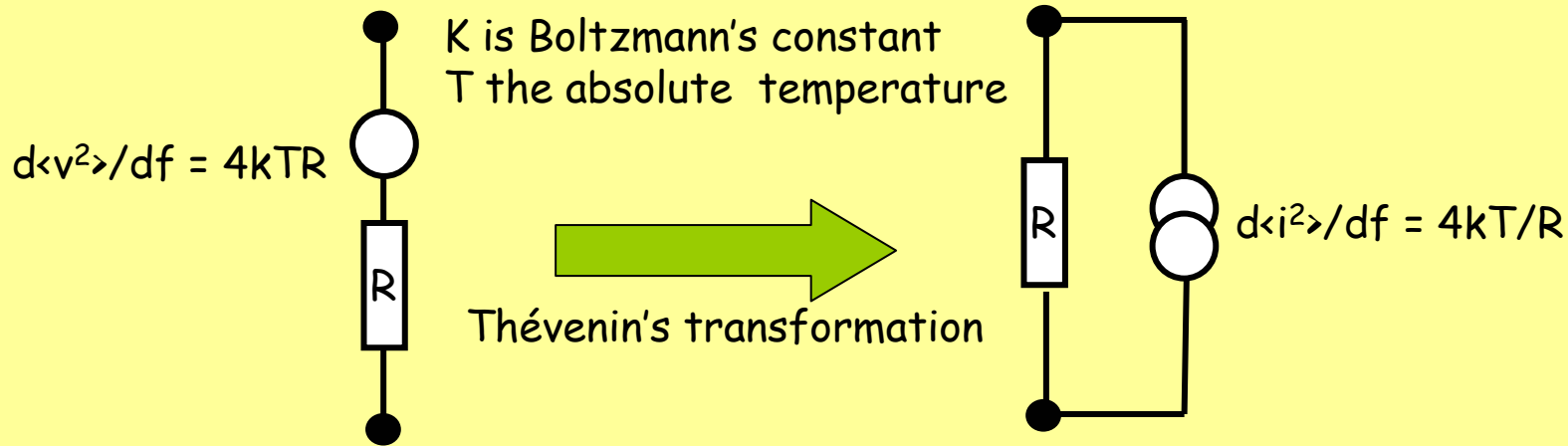
Which states that  $S(f)df$  represents the elementary contribution to the root mean square noise brought about by the spectral frequencies in the  $f, f+df$  interval.

The noise sources associated with electron devices are described by their spectral power densities. The noise power spectra plotted as functions of frequency provide the basic information about the features of each noise source. Among the sources, *of fundamental relevance is the one which describes the noise associated with the main current in an active device. This noise is usually referred to the input of the device and represented by a voltage source. Its spectral power density can be described as the sum of a frequency-independent (white) term and a term representing the so-called low-frequency noise which features its larger value at low frequencies and then decreases as  $f$  increases.*

## Thermal noise

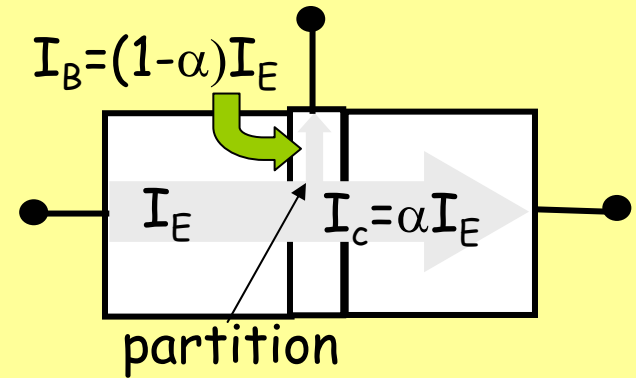
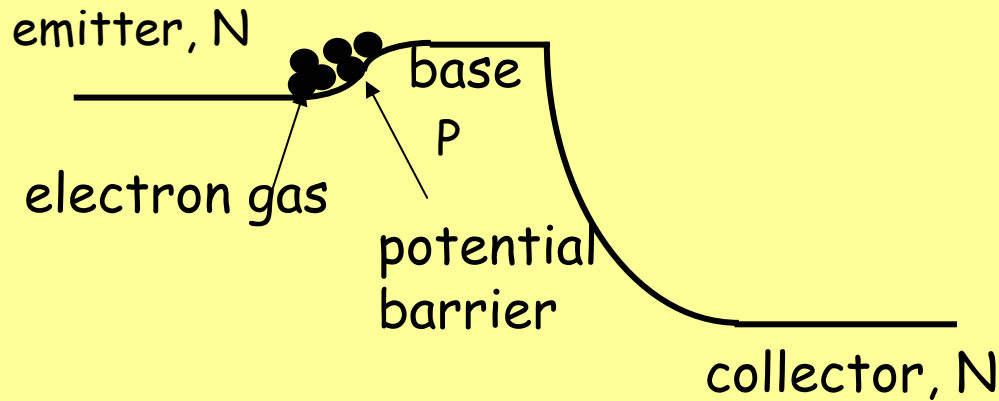
First observed by J.B. Johnson in metal resistors. Original paper:  
J.B. Johnson: Thermal agitation of electricity in conductors  
*Phys. Review, Vol 32, pp 97-109, July 1928*

The representation of thermal noise in a resistor is shown in the figure



- o Any resistor at thermal equilibrium (no current flowing through it) exhibits only thermal noise
- o A metal film resistor features only thermal noise even when current flows through it
- o A non metallic resistor through which current flows, besides thermal noise may exhibit the so called **excess noise** whose spectrum has an  $f^{-1}$  frequency dependence.

## Noise in bipolar transistors

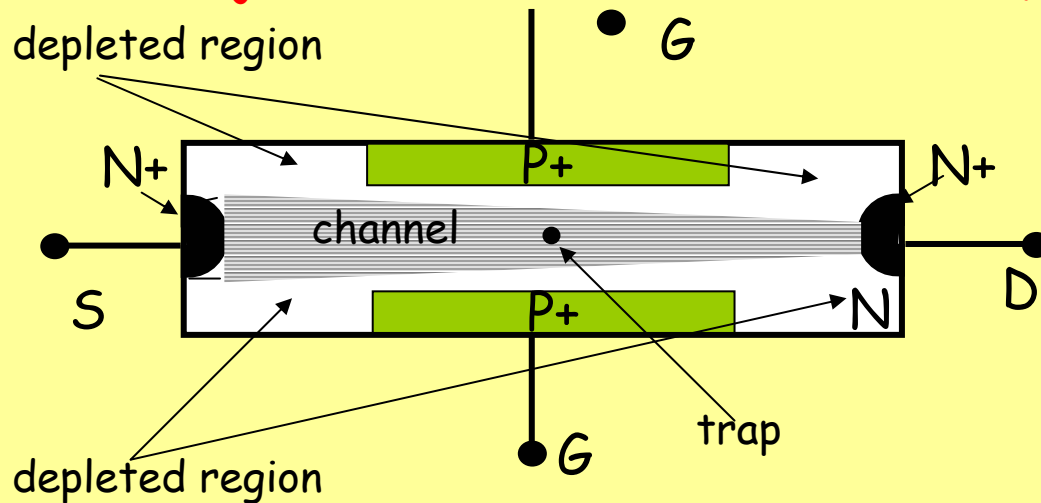


The electrons that in the unit of time jump over the potential barrier at the emitter-base junction constitute the emitter current. Such a current is affected by noise. To understand the reason, subdivide the time axis into equal elementary intervals  $\Delta t$ . The number of electrons  $\Delta n$  jumping over the barrier in  $\Delta t$  is a random variable. Such effect, called Shot Noise was first observed by Schottky in the current of a vacuum diode operating in the saturated region. The noise associated to the emitter current splits into a term associated with the collector current and one associated with the base current.

As the process of splitting is of random nature, an additional noise is present, called partition noise, which was first observed in the vacuum tetrode, a multigrad tube.

Nevertheless, the base-referred voltage source which describes the noise associated with the collector current **features the lowest spectral power density of all active devices at a given standing current.**

## Noise in junction field-effect transistors (JFET)



I like to quote here a sentence used by A.van der Ziel to settle a dispute about the nature of the noise in a junction field-effect transistor

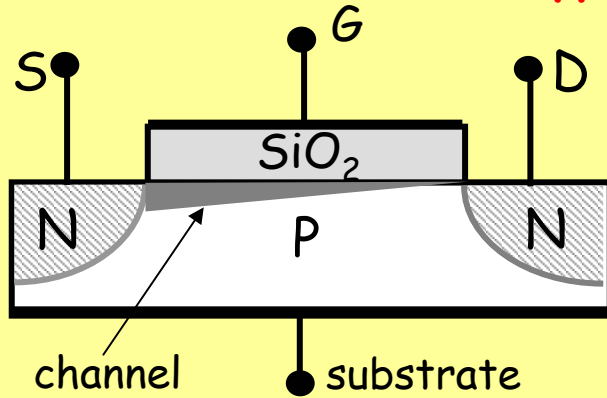
*It has been suggested that the observed noise can be interpreted as suppressed shot noise. There is no physical basis for such a suggestion. For evidently the field-effect transistor operated on the principle of true conductance modulation, as Shockley's theory indicates.*

***Generally one associates thermal noise with a true conductance and not shot noise. It is hard to see how shot noise could ever be generated.....***

The high frequency noise in a JFET has, accordingly, an  $f^0$  frequency dependence.

The low-frequency noise in a JFET is due to the trapping of the carriers by defects in the channel and their release after a random trapping time (Lorentzian noise). In practical cases it can be described by an  $f^{-2}$  frequency dependence. As the number of defects in the channel of a low-noise device is small, the JFET features the best low-frequency behavior of all field-effect devices, as clearly shown by the noise spectrum of the next page.

## Noise in enhancement-type mosfets



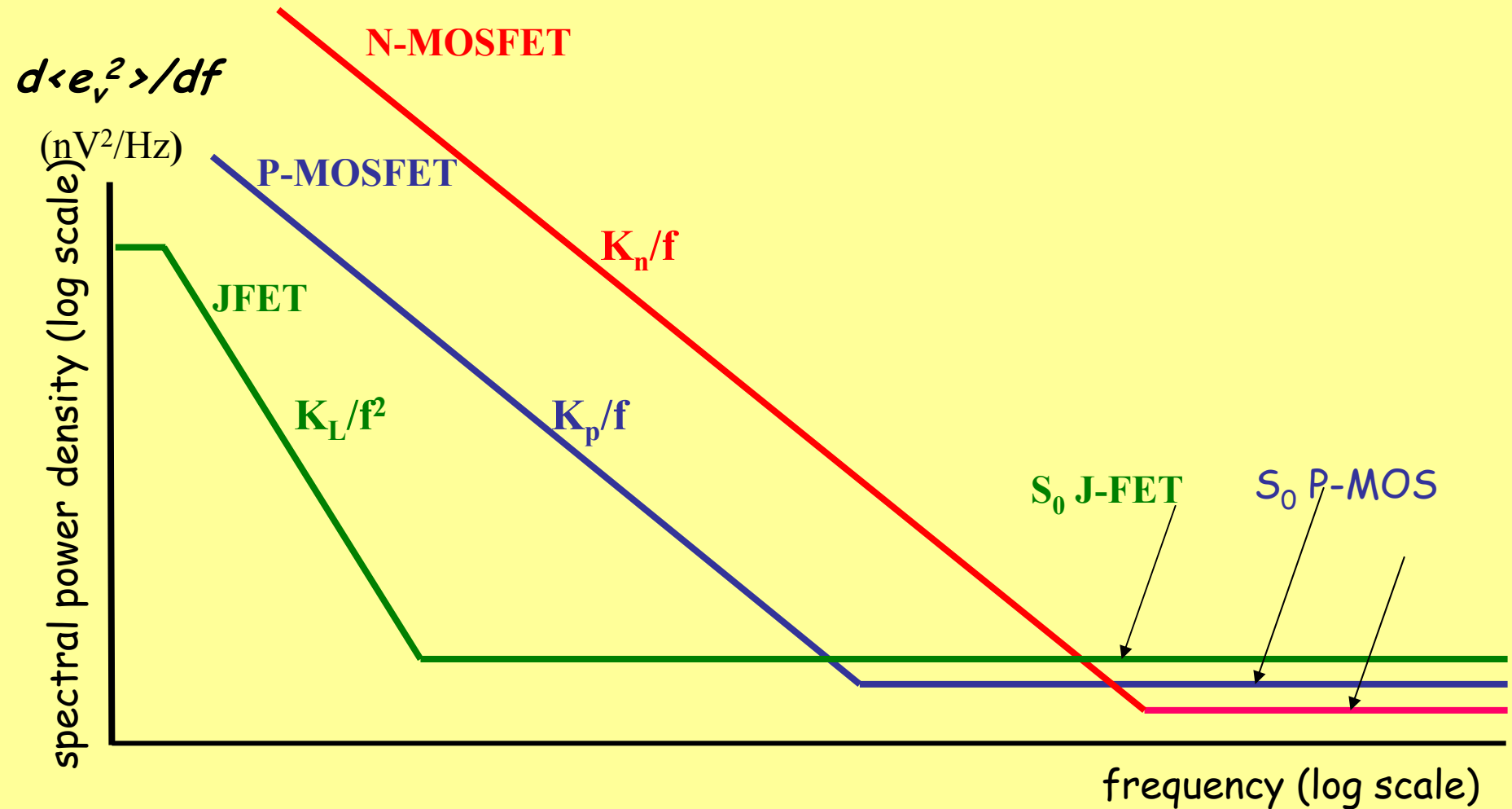
For the high-frequency noise in an enhancement-type mosfet the same argument used in the case of the JET leads to the conclusion that the noise is of thermal nature and that its frequency dependence is  $f^0$ .

The low-frequency noise mechanism in enhancement-type mosfets is related to the interaction of the carriers with traps in the gate-oxide or at the interface silicon-oxide.

A large amount of low-frequency noise with  $f^{-1}$  dependence is generated by this process, because of which enhancement-type mosfets for a long time have been considered unsuitable in radiation detector applications. Even now they are not employed in application where the noise of the front-end must be pushed down to the lowest possible limits.

However, there are some front-end problems where, the enhancement mosfets represent the only viable solution. ***This became clear when accelerator experiments moved from the extracted beam situation to the colliding beam case.*** The finely segmented vertex detectors employed for tracking purposes require front-end systems of high functional density, including multiplexing features to reduce the number of cables leaving the interaction regions.

Qualitative comparison of the frequency dependence of the spectral power density  $d\langle e_v^2 \rangle/df$  in three active elements of different nature





## Voltage-Sensitive or Charge-Sensitive preamplifier?

With detectors featuring a reliable in value and stable capacitance, solution A of the previous page is feasible. Configuration A was currently employed with ionization chambers. However, it can be employed also for instance with diamond ionization chambers and totally depleted semiconductor detectors that feature reliable and stable capacitances.

At the end of a very fundamental paper on a low-noise voltage-sensitive preamplifier for ionization chambers, Emilio Gatti and coworkers observed that the nature of the parameter to be measured, a charge, suggested the operational integrator as the most suitable solution. That remark clearly pointed to the charge-sensitive configuration. However, as Gatti recognized later, such a suggestion *had been given too early* and therefore went unnoticed.

Later, when semiconductor detectors went into use and the total depletion mode was ruled out by the limitations in the quality of the material, the charge-sensitive loop became essential.

To complete the answer to the question on top of the page it must also be pointed out that:

- o The **charge-sensitive preamplifier has a capacitive feedback** and with a suitable design of the charge restoration block (indeed a very critical point) is almost free from external sources of thermal noise. The voltage-sensitive solution has a resistive feedback, which adds to  $d \langle e_n^2 \rangle / df$  a thermal noise contribution approximately equal to  $4kTR_1$ .

- o In the **charge-sensitive loop** the risetime is proportional to  $C_d$ , while **in the voltage-sensitive circuit it** is independent of  $C_d$  and paradoxically shows a slight reduction as  $C_d$  is increased.

## Criteria for minimum noise operation

The spectral power density  $d\langle v_{p,n}^2 \rangle/df$  of the noise voltage at the preamplifier output has the following frequency dependence:

$d\langle v_{p,n}^2 \rangle/df = A_0 f^0 + A_1 f^{-1} + A_2 f^{-2}$  where the  $A_0, A_1, A_2$  coefficients have the following meaning:

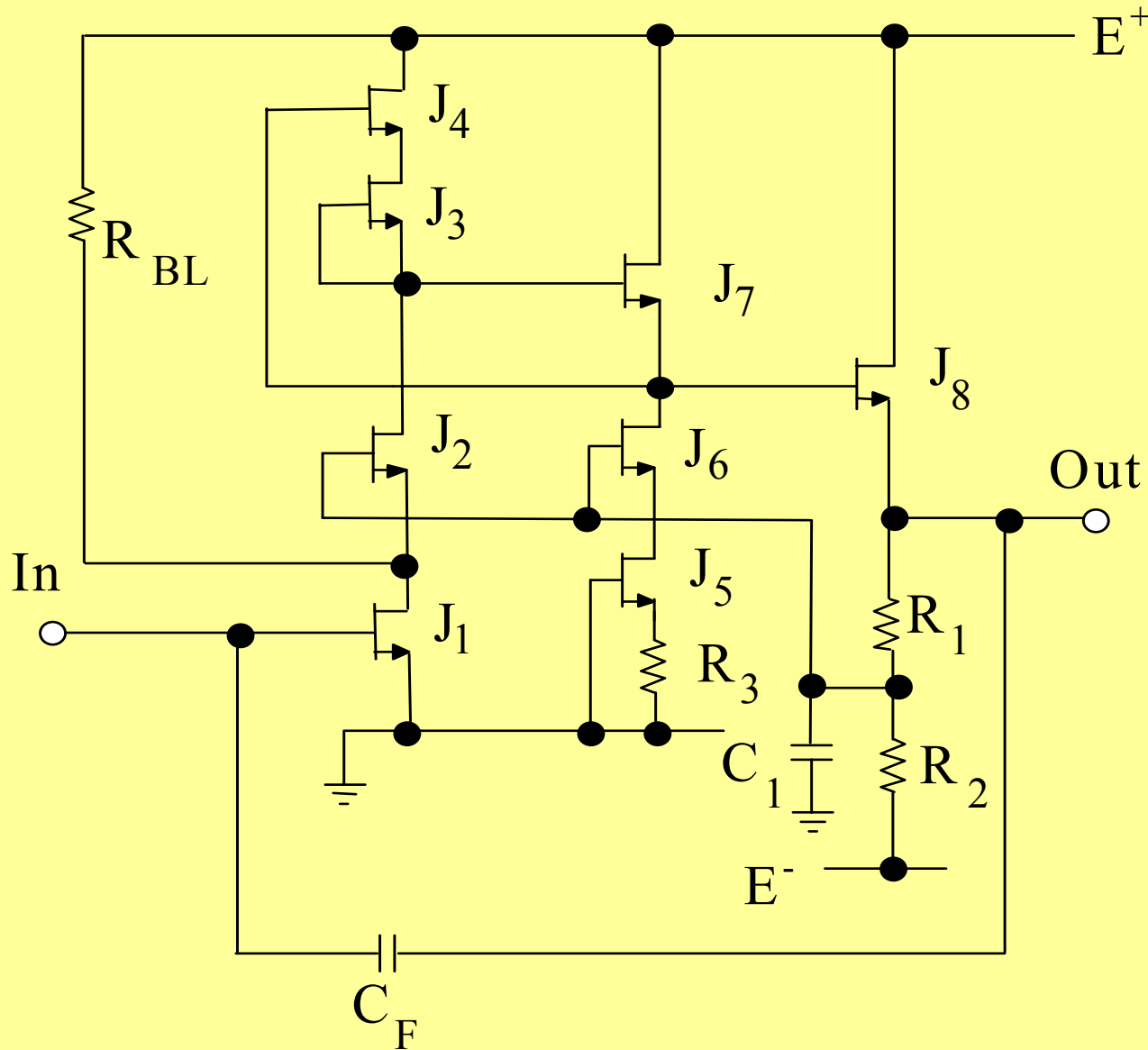
$A_0 f^0$  accounts for the high frequency noise in the active device at the preamplifier input, either the shot noise in the collector current of a bipolar transistor or the channel thermal noise in a JFET or a MOSFET.

$A_1 f^{-1}$  consists of two contributions. One is the low-frequency noise with spectral density  $f^{-1}$  in the channel current of field-effect devices, which is particularly important in enhancement-type MOSFETs. The second one is the noise associated with dielectric losses in the capacitors connected to the inputs of the preamplifiers. This noise is included in the current sources in of circuits A and B, where it is described by a spectral power density with  $f^1$  dependence.

$A_2 f^{-2}$  arises from the following sources:

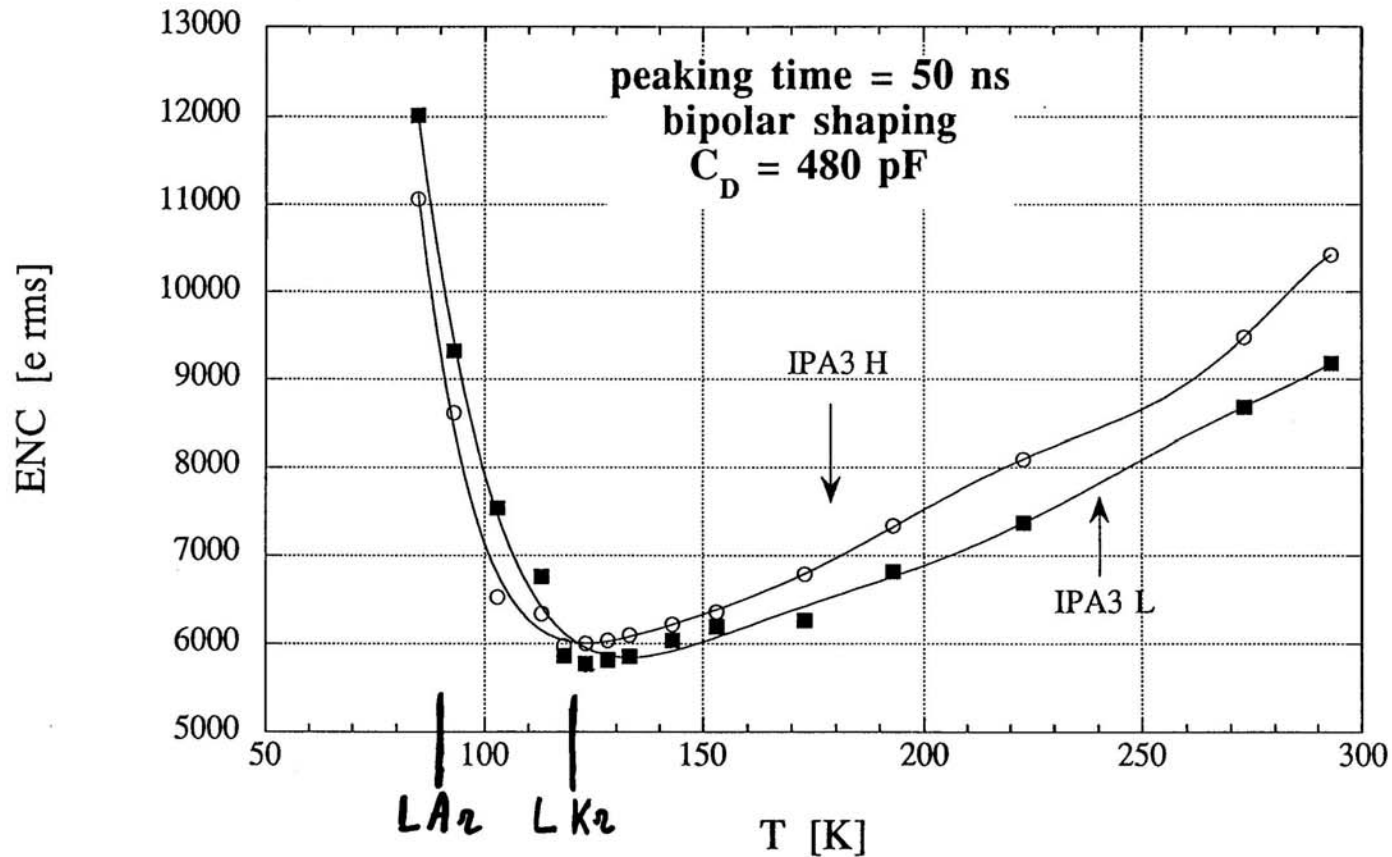
- the Lorentzian noise in the channel current of a JFET front-end device (an approximation).
- the white noise terms in the current sources  $i_N$ , that have the following origin:
  - a) the thermal noise in resistor  $R_B$  of circuit A
  - b) shot noise in the detector leakage current
  - c) shot noise in the input current of the front-end device, which is particularly important in the case of a bipolar transistor
  - d) shot or thermal noise in the restoration circuit of fig.B.

# ***Detectors operating at cryogenic temperatures and related front-end problems***



This circuit was developed as a collaboration INFN-Brookhaven Natl Lab in the framework of the ATLAS liquid Ar calorimeter R&D. It is entirely based upon N-channel JFETs belonging to a process of outstanding noise performances.

Temperature dependence of the noise charge for the All-JFET integrator based on the buried layer approach. The curves refer to two circuits of different channel doping (L and H materials). The attempt was to shift the condition at which the minimum occurs to lower temperatures.



GaAs MESFETs maintain good noise features at temperatures where Si JFETs fail, as pointed out by this table, which shows the values of channel noise in the amplifier at 77K and 89K. Besides, their 1/f-noise, which is large at room temperature, decreases constantly as the temperature is reduced.

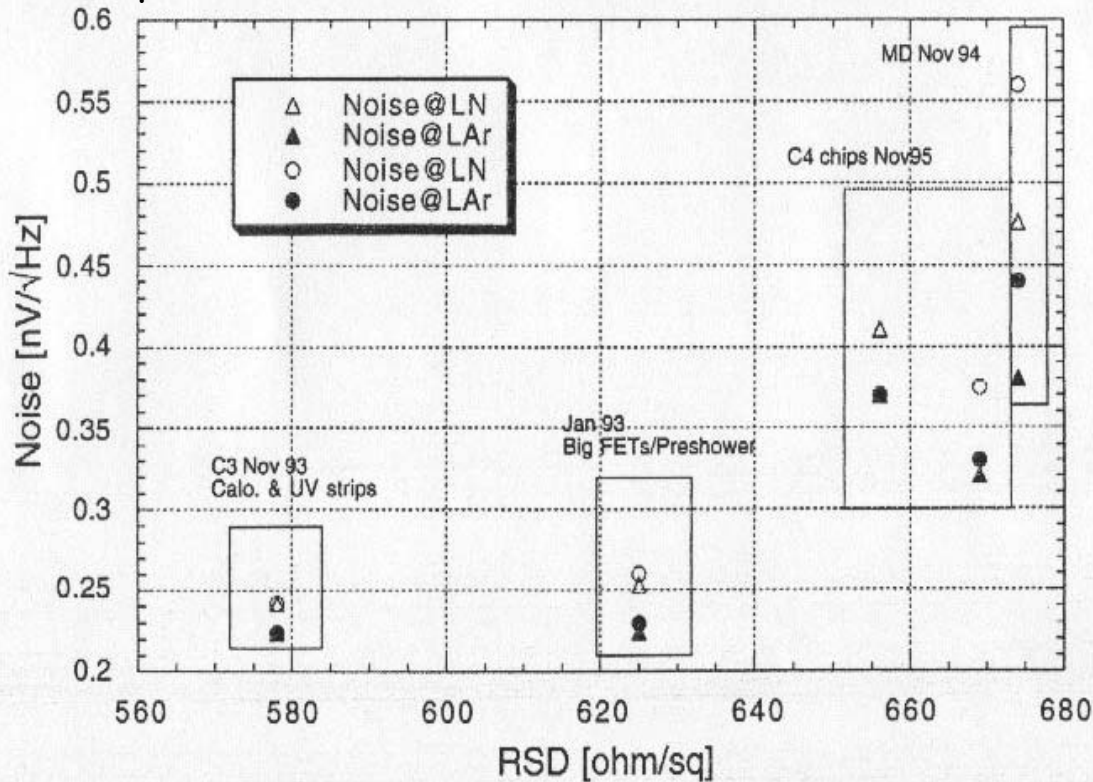


Fig. 6. Noise density of MESFETs made in various foundry runs, at 77 and 87 K as a function of channel resistivity.

## RESURRECTING THE GERMANIUM JFET?

The only device which may be able to operate over the entire cryogenic temperature range, including liquid He temperatures, while retaining a satisfactory noise behavior is the germanium field-effect transistor. This was confirmed thirty years ago in some preliminary tests, on devices fabricated with a technology that would be considered primitive by today's standards (1). The better behavior of germanium JFETs at low temperatures can be understood from TABLE I which compares the parameters determining the conductivity of germanium and silicon. Germanium has a much smaller ionization energies of the doping impurities than silicon, which results in a higher carrier density at low temperatures. The smaller effective mass of the carriers in germanium also contributes to yield a higher mobility.

TABLE I

	Energy gap (eV)		Ionization energy of impurities		Effective mass ratio $m^*/m_0$	
	0 K	300 K	P	B	holes	electrons
Ge	0.744	0.67	0.012	0.0104	0.37	0.55
Si	1.153	1.107	0.044	0.046	0.59	1.1